www.coinweb.no

SINTEF Building and Infrastructure Stefan Jacobsen, Jon Håvard Mork, Siaw Foon Lee , Lars Haugan

Pumping of concrete and mortar – State of the art

COIN Project report 5 - 2008

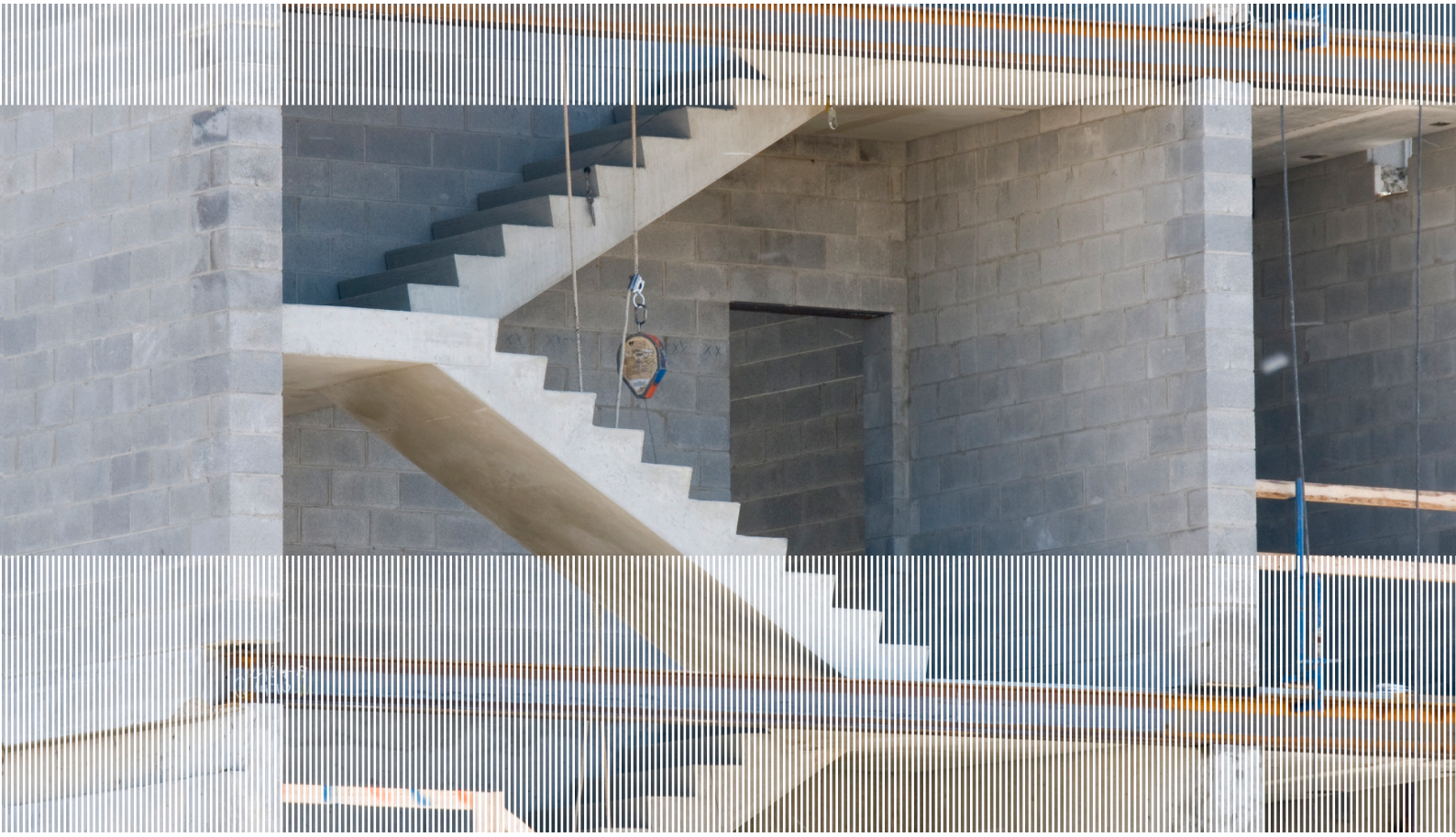

SINTEF

SINTEF Building and Infrastructure

Stefan Jacobsen (NTNU), Jon Håvard Mork (maxit Group),
Siaw Foon Lee (NTNU), Lars Haugan (SINTEF)

Pumping of concrete and mortar – State of the art

COIN P2 Improved construction technology

SP 2.4 Workability

COIN Project report 5 – 2008

COIN Project report no 5
Stefan Jacobsen (NTNU), Jon Håvard Mork (maxit Group),
Siaw Foon Lee (NTNU), Lars Haugan (SINTEF)
Pumping of concrete and mortar – State of the art
COIN P2 Improved construction technology
SP 2.4 Workability

Keywords:
Materials technology, concrete, Pumpability, Rheology, Rheology, Flow

ISSN 1891–1978 (online)
ISBN 978–82–536–1069–6 (pdf)

Address: Forskningsveien 3 B
POBox 124 Blindern
N-0314 OSLO
Tel: +47 22 96 55 55
Fax: +47 22 69 94 38 and 22 96 55 08

www.sintef.no/byggforsk
www.coinweb.no

Cooperation partners / Consortium Concrete Innovation Centre (COIN)

Aker Solutions
Contact: Jan-Diederik Advocaat
Email: jan-diederik.advocaat@akersolutions.com
Tel: +47 67595050

Borregaard Ligno Tech
Contact: Kåre Reknes
Email: kare.reknes@borregaard.com
Tel: +47 69118000

maxit Group AB
Contact: Geir Norden
Email: geir.norden@maxit.no
Tel: +47 22887700

Norcem AS
Contact: Terje Rønning
Email: terje.ronning@norcem.no
Tel: +47 35572000

NTNU
Contact: Terje Kanstad
Email: terje.kanstad@ntnu.no
Tel: +47 73594700

Rescon Mapei AS
Contact: Trond Hagerud
Email: trond.hagerud@resconmapei.no
Tel: +47 69972000

SINTEF Building and Infrastructure
Contact: Tor Arne Hammer
Email: tor.hammer@sintef.no
Tel: +47 73596856

Skanska Norge AS
Contact: Sverre Smeplass
Email: sverre.smeplass@skanska.no
Tel: +47 40013660

Spenncon AS
Contact: Ingrid Dahl Hovland
Email: ingrid.dahl.hovland@spenncon.no
Tel: +47 67573900

Norwegian Public Roads Administration
Contact: Kjersti K. Dunham
Email: kjersti.kvalheim.dunham@vegvesen.no
Tel: +47 22073940

Unicon AS
Contact: Stein Tosterud
Email: stto@unicon.no
Tel: +47 22309035

Veidekke Entreprenør ASA
Contact: Christine Hauck
Email: christine.hauck@veidekke.no
Tel: +47 21055000

Summary

The pumpability of concrete, or its ability to move through pipes and hoses by the help of a pump while maintaining its fresh and hardened properties, can be quantified as being better the lower the necessary pressure to obtain a given flow in a specific configuration and set-up (pump type, -capacity, pipes/hoses, –diameter/length etc). The practical pumping process including the principles of piston- and screw pumps show that for a wide range of concretes the flow in a given set-up is approximately proportional to pump-frequency whereas resulting pressure depends on concrete technological parameters (concrete composition, rheology). Based on review and some preliminary pumping trials in the NTNU concrete laboratory we propose concrete pressure gradient over the pipe length as a measure of pumpability for a given pump set-up.

We then present some results on flow measurements in experiments on commercial premix products and open lab concretes and mortars. Measurements of rheological parameters in the BML-viscometer, concrete pressure in pipe , concrete flow and energy in an instrumented full-scale pump-set up with a screw pump indicate that plastic viscosity is the main rheological parameter affecting pumpability. Analysis of the degree of plug flow indicates a wide variety of flow profiles. A simplified 2D FEM analysis with Navier Stokes equation using Papanastasious solution for Bingham fluid gives convergent flow with similar plug flow profiles as the analytical Buckingham Reiner equation. An analytical slip layer model was developed applying the Bingham model. It can be fitted to plug flow but more experiments are needed on what the boundary flow looks like.

Continued research should study plug flow, slip layers and concrete rheology effects (admixtures, matrix volume and –properties) on pumpability including effects of pump frequency, increasing vs decreasing flow, hose characteristics (material, diameter, length, height etc). This could also be used in form filling experiments. A reliable numerical model must describe both flow through the pump and pipes/hoses as well as the form filling satisfactorily.

Oslo, 2008

Tor Arne Hammer

Stefan Jacobsen (NTNU)
Jon Håvard Mork (maxit Group)
Siaw Foon Lee (NTNU)
Lars Haugan (SINTEF)

Foreword

COIN - Concrete Innovation Centre - is one of presently 14 Centres for Research based Innovation (CRI), which is an initiative by the Research Council of Norway. The main objective for the CRIs is to enhance the capability of the business sector to innovate by focusing on long-term research based on forging close alliances between research-intensive enterprises and prominent research groups.

The vision of COIN is creation of more attractive concrete buildings and constructions. Attractiveness implies aesthetics, functionality, sustainability, energy efficiency, indoor climate, industrialized construction, improved work environment, and cost efficiency during the whole service life. The primary goal is to fulfill this vision by bringing the development a major leap forward by more fundamental understanding of the mechanisms in order to develop advanced materials, efficient construction techniques and new design concepts combined with more environmentally friendly material production.

The corporate partners are leading multinational companies in the cement and building industry and the aim of COIN is to increase their value creation and strengthen their research activities in Norway. Our over-all ambition is to establish COIN as the display window for concrete innovation in Europe.

About 25 researchers from SINTEF (host), the Norwegian University of Science and Technology - NTNU (research partner) and industry partners, 15 - 20 PhD-students, 5 - 10 MSc-students every year and a number of international guest researchers, work on presently 5 projects:

- Advanced cementing materials and admixtures
- Improved construction techniques
- Innovative construction concepts
- Operational service life design
- Energy efficiency and comfort of concrete structures

COIN has presently a budget of NOK 200 mill over 8 years (from 2007), and is financed by the Research Council of Norway (approx. 40 %), industrial partners (approx 45 %) and by SINTEF Building and Infrastructure and NTNU (in all approx 15 %). The present industrial partners are:

Aker Kværner Engineering and Technology, Borregaard LignoTech, maxit Group, Norcem A.S, Norwegian Public Roads Administration, Rescon Mapei AS, Spenncon AS, Unicon AS and Veidekke ASA.

For more information, see www.coinweb.no

Table of contents

1 Introduction - pumpability

The pumpability of concrete has been defined as its ability to flow through a pipe by the help of a pump (ACI 1998), and also the ability of confined concrete to flow under pressure while maintaining its initial properties (Jolin et al 2006). Some examples of low pumpability due to lack of maintenance of initial properties are forward segregation in the pipe leading to blocking, negative effects on air void content and –structure, as well as reduced compressive strength compared to concrete that has not been pumped. Due to varying pump-and-pipe configurations from one site to another (capacity, pipe length, -height, -diameter, -material etc), the term pumpability yields for a site-specific pump set-up. Quantification of pumpability of a concrete mix should therefore be obtained by resulting flow or pressure of fresh conrete, or pumping energy required for the specific mix in the actual set-up. Pumpability may also be described more qualitatively in terms of ease or problems with pumping operations from proportioning, grouting of pipe lines, pump trials, blocking etc. Pumping of concrete and mortar is a cost effective way of industrializing the construction industry as indicated by present market figures. In Norway approximately 50 % of the concrete is pumped at some stage of the placing process (Fabeko 2007, www.fabeko.no). In addition mortars, grouts etc are pumped, often in a combined premix silo/continuous mixer/pump system. Obviously most concretes today are pumpable. There are, however, certain types of concretes where pumpability is still not completely resolved. Examples are slab-on-grade (K Tuutti pers comm. Oct 2007), certain light weight aggregate concretes, (EuroLightcon 2000), possible uncontrolled increase of pressure during high speed pumping of certain self compacting concretes (DeSchutter, personal communication December 2007), fibre concrete with uncontrolled fiber orientation etc. To proceed in the development of pumpable concrete we have reviewed pumping and investigated rheological properties and compositions important for pumpability quantified as concrete flow, -pressure and pump energy consumption. We also conducted some preliminary tests on the effect of concrete rheology on pumpability, the effect of pumping on rheological properties of concrete as well as effects on hardened properties such as strength, homogeneity and air void content. Finally we look at some simplified ways of modelling the pumping process.

2 Concrete pumping

2.1 Piston pumps

Piston pumps dominate the concrete industry due to their high capacity. Figure 1 below shows an example with two pistons working by filling one while emptying the other via a valve shifting opening towards the feeder and shutting towards the pipe.

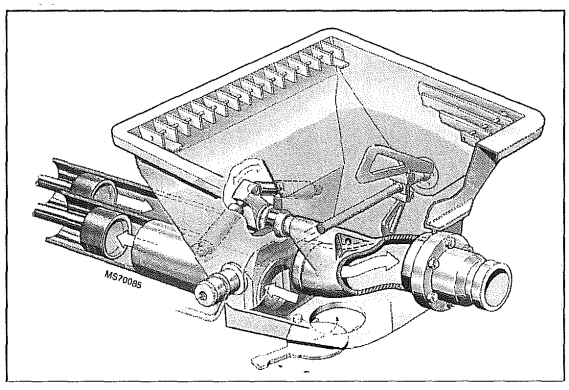

Figure 1. Piston pump with valve letting concrete in from hopper to one piston and out to tube from the other piston alternating with the strokes of the two pistons (www.Putzmeister.com)

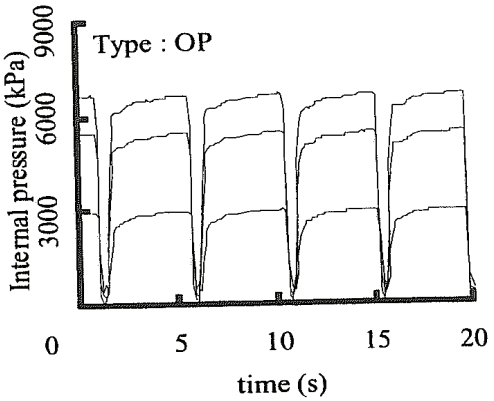

Figure 2. Typical concrete pressures along pipe (3 points) with max pressure near pump and alternating according to the frequency of the pump (Watanabe et al 2001)

The pressure in the concrete shifts with the frequency of the strokes of the pump, see figure 2 above. The maximum concrete pressure can become quite high and even higher than the 7 MPa shown in figure 2. The minimum pressure at retreat of piston before closure of valve and opening for stroke of the other piston can even be negative. In figure 3 below the suction is seen to be very strong so as to possibly reverse the flow in pace with the pump frequency. Clearly this will affect the flow conditions both locally and globally in the pipe. The measured pressure gradient over the length of the pipe is normally linear, as seen in figure 4.

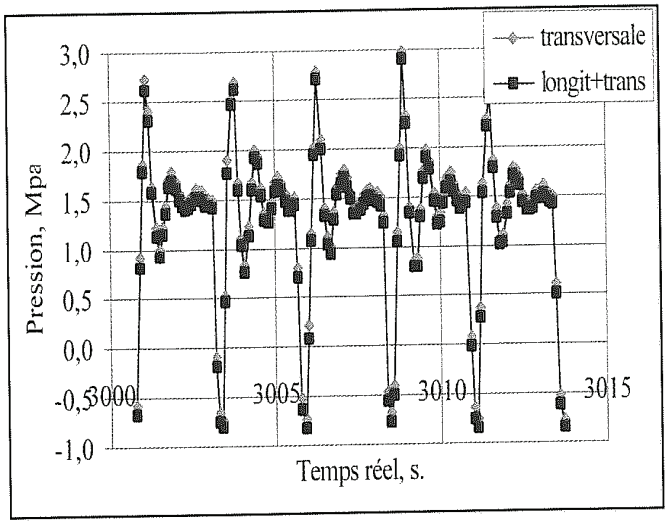

Figure 3. Suction in fresh concrete in pipe observed at the turn of the stroke of a piston pump (Kaplan 2001)

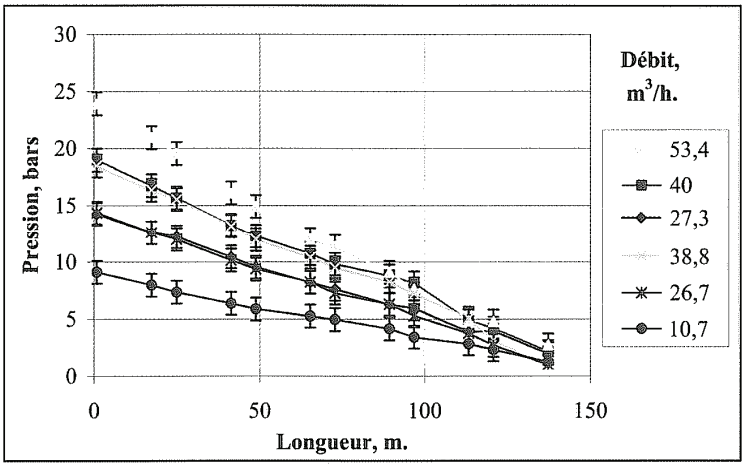

Figure 4. Pressure gradient along steel pump pipe for different concrete mixes pumped with piston pump (Kaplan 2001)

2.2 Screw pumps

The screw- (or worm-) pump works by screwing the concrete forward by means of a steel screw inside a rubber stator with conveying chambers between the steel and the rubber, see figure 5. In addition there is usually a screw at the bottom of the feeder moving the concrete towards the entrance of the stator. The conveying chamber is continuously moving forwards between the steel screw and the rubber stator, sucking in concrete from behind and pushing it out into the hose in front, figure 5. Concrete flows into the pump by the suction created by the forward moving conveying chamber, additional hydrostatic pressure from the depth of the concrete in the feeder and the concrete flow towards the rotor/stator inflow caused by an additional screw feeder at the

bottom of the hopper. Figure 6 shows capacity and energy use vs. concrete pressure. Both figures, courtesy maxit Group AB R&D/m-Tec (Mork 2007a)

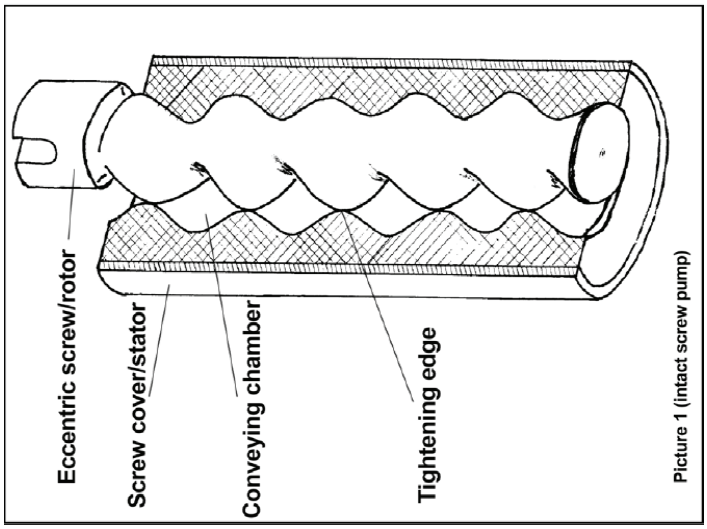

Figure 5. Screw pump with steel rotor and rubber stator, concrete entering at left and conveyed via moving conveying chamber (maxit Group/m-Tec)

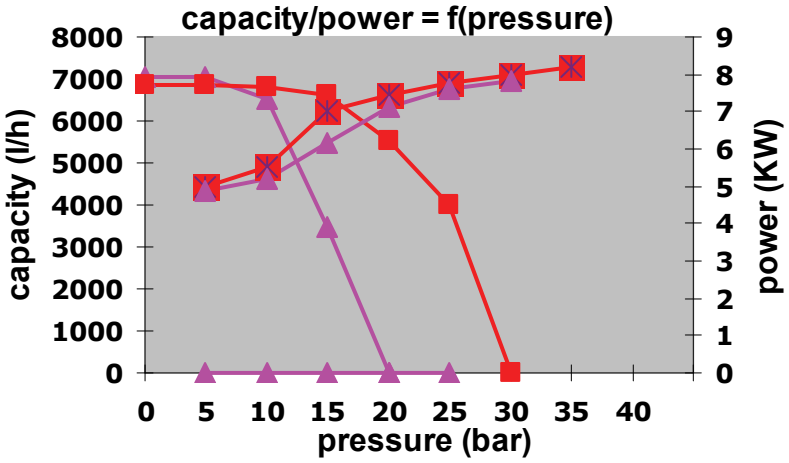

Figure 6. Concrete flow and energy consumption in screw pump as function of concrete pressure for two different materials (maxit Group/m-Tec)

The capacity of screw pumps is generally lower than that of piston pumps, but the equipment is lighter and easier to handle. The pump used for the preliminary experiments given later on in this report has a maximum capacity of about 7 m^3/h at 50 Hz and 45 mm hose diameter with length 26,6 m. Depending on the material, the flow out of the pump seems to reach some kind of threshold beyond which the capacity is reduced as the pressure increases, see figure 6. Even by almost doubling the energy consumption, it is usually not possible to keep up the capacity due to backflow as the pressure rises on the downstream side of the pump and the relatively soft rubber in the stator cannot withstand the downstream pressure. The effect seems to be depending on the material, as seen in figure 6 for two different cement based materials tested by maxit Group.

For both piston- and screw pumps we may thus assume that the flow out of the pump is constant and depends primarily on the pump frequency (rotations or strokes per unit time). The pressure in the fresh concrete in the hose will primarily depend on the rheological properties of the concrete and the conditions in the pipe (length, diameter, geometrical configuration, friction). Due to the steady screwing the pressure is constant without the alternation seen with a piston pump, see also figure 5 in section 5 and earlier findings (Mork and Jacobsen 2008).

3 Concrete pumpability related to consistency and rheology

3.1 Practical approach

Two basic properties of pumpability are (Spiratos et al 2003); 1) sufficient paste content so that there is enough grout for a slip layer, 2) suitable grout consistency and structure between aggregate grains to hinder forced or pressurized bleeding due to pump pressure. Thus we should look for ways to obtain suitable consistency, combined with resistance against squeezing out of water from the concrete due to the high pressure in the pipe or hose, so called pressurized bleeding (Wallevik 2002).

Abrams slump cone from 1913 is still the most used workability test at the building site, varying somewhat depending on the concrete workability: VeBe-time for stiff plastic consistency, slump for more or less plastic consistency and slump flow and flow time (T_{500}) for self compacting concrete (SCC). Slump is the simplest test to describe concrete pumpability (Stephenson 1968, Sakuta et al 1989, ACI 1998). One early recommendation was that slump < 50 mm gave unpumpable concrete, slump 50 – 100 mm ensures pumpability whereas slump > 100 mm gives unpredictable pumpability (Stephenson 1968). Empirical diagrams exist for designing the capacity of pumping equipment. This includes selection and design of pump and pipes including line diameter, -length and –pressure. The concrete slump has been the main rheological parameter. It has been used to characterize resulting pressure gradient as function of pump flow for varying pipe diameters, -length and –materials, see for example (Sakuta et al 1989, ACI 1998, Kaplan 2001). Figures 7 and 8 show such empirical relations between slump and pumpability.

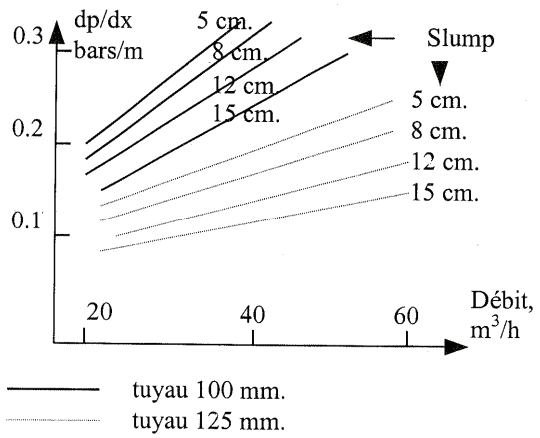

Figure 7. Effect of concrete slump on dp/dx as function of flow for different pipe diameters (Sakuta et al 1989). We postulate better pumpability the lower dp/dx for a given flow without negative effects on the concrete

In the nomogram in figure 8 (ACI 1998) a similar relationship is obtained, but it contains more necessary information embedded in a practical manner taking into account the effect of pipe material (rubber giving 3 times the pressure of steel), number and different types of curves (increasing the pressure), vertical sections etc.

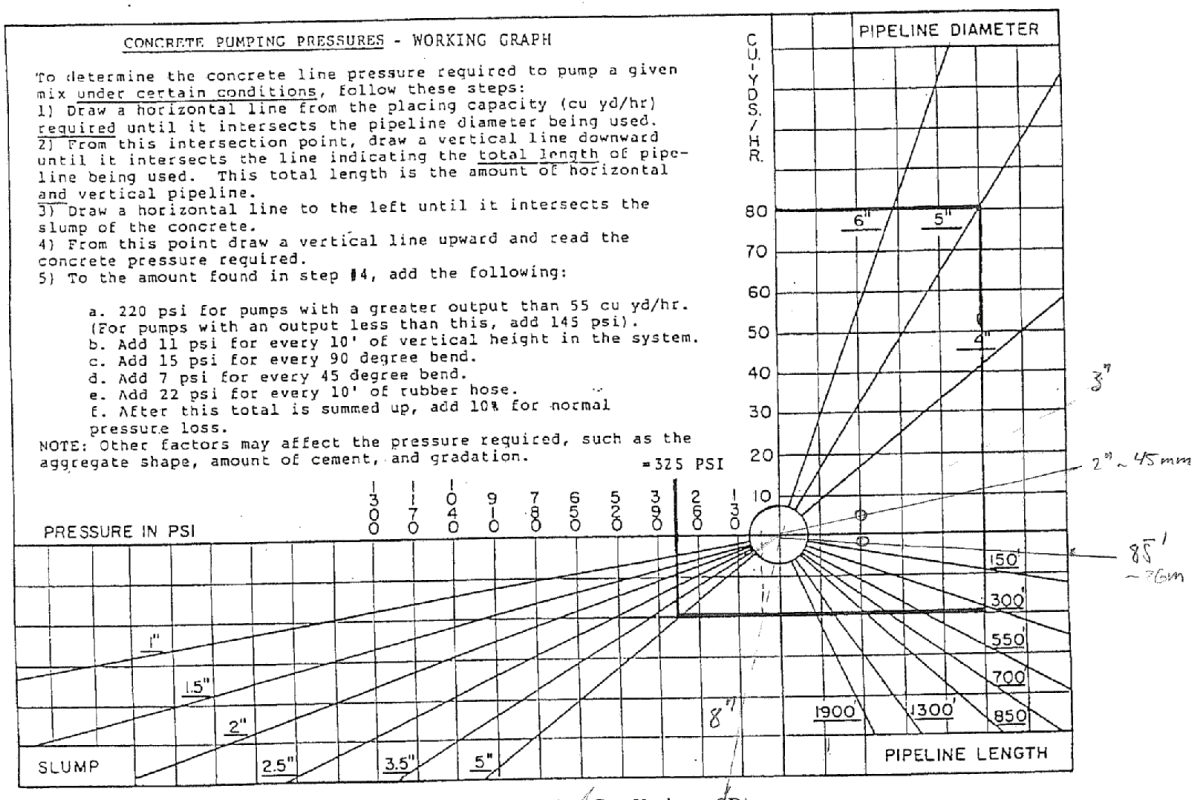

Figure 8. Diagram for dimensioning concrete pumping set-up including effect of concrete slump on pumpability (ACI 1998)

The rate of bleeding has been found to be a major factor for pumpability (Browne and Bamforth 1977, Tattersall and banfill 1983, Kaplan 2001, Kaplan and deLarrard 2005). High bleeding rate may cause water to be easily squeezed out and cause blocking. Increased bleeding due to the pressure in the pump and pipe has, as mentioned, been termed pressurized bleeding (Wallevik 2002). The testing and control of pressurized bleeding has been proposed as pumpability criterion (Browne and Bamforth 1977, Kaplan 2001) together with slump since the latter obviously is an insufficient measure of pumpability. Pressurized bleeding was measured in a special test cell as volume water squeezed out from a sample of fresh concrete at 3.5 MPa pressure after 10 and after 140 seconds; V_{10} and V_{140}. Figure 9 from (Browne and Bamforth 1977) shows acceptable combinations of ($V_{140} - V_{10}$) and slump to ensure adequate pumpability.

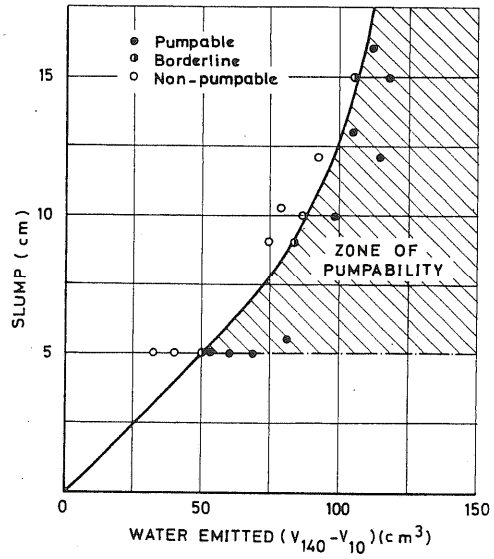

Figure 9. Pumpability as function of slump and bleeding (Browne and Bamforth 1977)

For materials with too low workability and too high pressurized bleeding, the resulting blocking of the coarse aggregate depends on the impulse of the piston pump, paste viscosity etc. This was described and quantified (Kaplan 2001, Kaplan and deLarrard 2005). They developed a more practical bleeding test using the standard pressurized air-void apparatus for routine testing of air void content in fresh concrete. They recommended that bleeding should be measured over a longer period than recommended in (Browne and bamforth); up to 60 minutes since it may take some time from mixing until pumping. They expressed the rate of bleeding in cm^3/hour, and based on full-scale pumping experiments they recommended a bleeding rate lower than approximately 20 cm^3/hour measured under pressure in the air void apparatus to ensure pumpability, see figures 10 and 11 below.

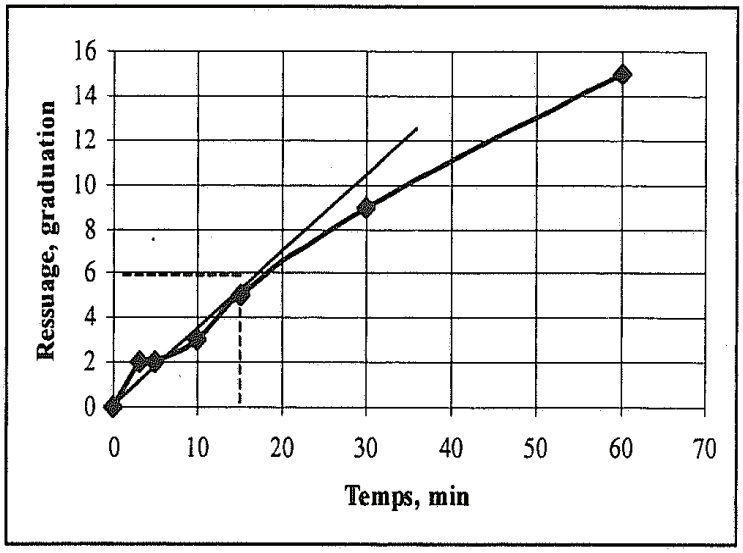

Figure 10. Bleeding (cm^3) vs time, 5 litres of concrete in standard air void apparatus (Kaplan 2001)

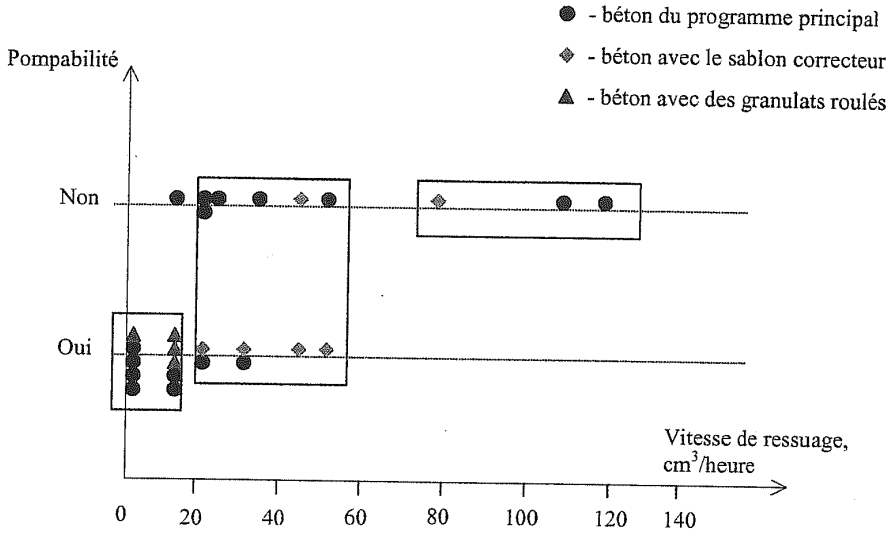

Figure 11. Limits for pumpability as function of bleed rate (cm^3/h) (Kaplan 2001)

For self compacting concrete (SCC) other practical tests than the original Abrams slump cone must be used. At the construction site, Slump-flow and T_{500} seem to dominate. A reinforcement J-ring can be used to indicate the ability of the SCC to pass reinforcement bars. In addition, test methods like V-funnel test, L-box test and sieve segregation resistance exist (Barthos et al 2002, European Guidelines for SCC 2005, Norsk betongforening 2007). It appears, however, that no criteria for pumpability of SCC based on these tests exist (Watanabe et al 2001, Lu, Laijun 2005, Feys, DeSchutter et al 2007). This is partly caused by the varying conditions in varying pump set-ups. The flow conditions in the pipe are for example unknown; in particular the flow profile. In

the research work on pumping of concrete (Rössig 1974), observations of flow profiles were made by pumping coloured concrete into un-coloured concrete and letting it harden. Similar studies and observations have been made in Russia and referred in (Kaplan 2001). From figure 12 below, it seems that a flow profile with some kind of slip layer exists for a stiff-plastic concrete, having around 40 cm flow spread measured with the German DIN-test.

Figure 12. Flow profiles observed after pumping concrete into coloured concrete, 40 cm flow-spread concrete pumped at 1.77 m/s flow rate in 125 mm steel pipe (Rössig 1974)

The existence of a slip layer has also been discussed by several (Tattersall & Banfill 1983, Kaplan 2001, Haist & Muller 2005). The latter study extracted the pumped material near the wall, measured its rheological properties and concluded that there is such a slip layer. There could be several reasons for a paste- or matrix rich layer at the wall: one being the kind of dynamic segregation (Thrane 2007 p.53). Apparently, coarse particles in a fluid matrix tend to migrate towards the centre, that is; towards minimum rate of shear. For concrete pumped in a pipe, this means towards the centre where the shear rate is zero or shifting. In an ongoing work (Kalogiannidis 2008), a similar approach has been taken as in (Rössig 1974) on modern, self compacting materials. Preliminary studies of SCC mortar or mini concretes with 8 mm maximum aggregate size have shown that in plastic pipes (Ø = 45 mm) with expected low friction, clear flow profiles can be seen even at low flow velocities < 0.5 m/s (Kalogiannidis 2008).

3.2 Rheological approach

More advanced rheological measurements on fresh concrete exist based on that concrete can be treated as a Bingham fluid. Using a viscosimeter, the Bingham material parameters plastic viscosity μ, and yield shear τ_0 (see appendix 1), which govern the flow in a pipe, can be measured. The Bingham model is very useful even though it does not describe such phenomena as non linearity during movement (shear thinning/-thickening and thixotropy) (Helland 1982, Mork 1994). The viscosimeters in the NTNU concrete laboratories have been further developed from its predecessor (Tattersal 1976). The BML viscosimeter has been used extensively for more than a decade to study μ and τ_0 (Wallevik 1990, Wallevik & Gjørv 1990, Barthos et al 2002), and is now in commercial use in many concrete laboratories. Relations have been found between slump and yield strength and between flow and plastic viscosity (Hu, deLararrd 1996, Sedran and deLarrard 1999, Wallevik C&CR 2006). The fluid flow conditions in the coaxial viscosimeter have also been studied experimentally and numerically in great detail (Wallevik 2003).

Even though the flow during the coaxial movement of the viscosimeter is different from the flow in a pipe, it is reasonable to assume that it can be used to evaluate the pumpability of a concrete mix before full scale pumping is carried out. The first large scale study of the concrete Bingham parameters as measured in a coaxial viscosimeter (and also slump) vs. pumpability, measured as pressure in the hydraulic oil of a concrete piston pump, were made on the very flowable high performance concrete (slump 190 - 240 mm) for the Gullfaks C Condeep platform (Hansen 1988). The investigated 2.7 m^3 concrete batches had w/b in the range 0.42-0.45 with 420 kg of

cement, 2 % silica fume and around 1.2 % superplastcizer by weight of cement. The results showed that both yield strength and plastic viscosity related to the hydraulic oil pressure. Increasing yield strength gave the best relation to increasing pressure. Also increased slump showed a relation to reduced pressure. Yield strength increased due to pumping and gave improved stability as observed from viscosimeter measurements made before and after pumping. It seems that the rheological data obtained before pumping correspond best to the measured pump pressures in the long pipeline, rising more than 180 metres vertically in the shafts of the large concrete structure. It was recommended that pumpable concrete should have as low yield strength and plastic viscosity as possible without loosing stability. Furthermore, largest effect of rheology on pumpability was expected for small pipe diameter, high pump flow and horizontal pipes with many bends. Later studies on-site of the Bingham parameters vs. concrete pressure measured in piston pumping were made in (Hu and DeLarrard 1996). The Bingham parameters were measured with a BTHREOM viscosimeter and showed essentially the same as was found earlier in (Hansen 1988) on a similar number of mixes.

Since the pressure- and movement conditions in a pipe, particularly with piston pumps, alternate as discussed above, it seems probable that the complete shear rate vs. shear cycle is of interest. The hysteresis observed during BML-viscosimeter testing, see figure 13, will probably affect flow and pressure in the pipe depending on pressure/suction and the local rate of shear in the flow profile. For piston pumps, where the shear may be changing constantly due to the alternation of the pump (see figures 2 and 3), the complete test cycle should therefore be investigated when comparing pumpability with viscometer measurements.

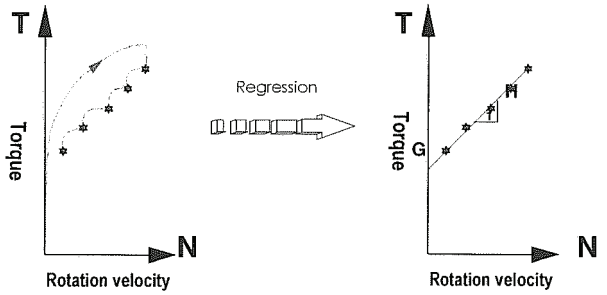

Figure 13. Hysteresis between increasing and decreasing rotation velocity in the coaxial BML-viscosimeter (Barthos et al 2002)

In a preliminary study of pump flow and pressure in screw pumps as related to rheology, we compared a simplified Hagen Poiselle Bingham fluid without plug flow with some measurements on pump flow, -pressure and rheology performed on the same materials (Jacobsen and Mork 2007). The expression in eq. (1) was used (Jacobsen and Mork 2007)[1] by integrating eq. (A5) in Appendix 1 ignoring the formation of a plug. This is a simplified integration termed $v(r)_{no\text{-}plug}$ in appendix 3 and 4 compared to the Buckingham Reiner equation, see eq. (A9) in appendix 1 and velocity distribution $v(r)_{plug}$ in appendix 3 and 4:

$$\frac{dp}{dx} = \frac{8\mu G_x}{\pi a^4} + \frac{8\tau_0}{3a} \Leftrightarrow G_x = \frac{\pi a^4}{8\mu}\left(\frac{dp}{dx} - \frac{8\tau_0}{3a}\right) \quad (1)$$

τ_0: yield shear strength [Pa]
μ: plastic viscosity [Pa·s]
dp/dx: pressure gradient (Pa/m)
a: tube radius [m]
G_x: total concrete flow [m^3/s] towards falling pressure gradient

[1] Note; error in equation in (Jacobsen and Mork 2007) is corrected in eq.(1), see also appendix 1.

The simplification of omitting the plug compared to eq.(A9) may result in "inward plugs" as seen in appendix 3. However, based on some excel-exercises with varying combinations of realistic pipe radii, plastic viscosities and yield strengths, it was found that the contribution from τ_0 in eq.(1) can be ignored for highly flowing concretes with low τ_0. Therefore, eq.(1) may be used as a simplified indication of pumpability as function of concrete rheology, pipe diameter and pipe length. Figures 14 and 15 below show the kind of relations eq.(1) give between diameter of pipe, plastic viscosity, flow and pressure gradient.

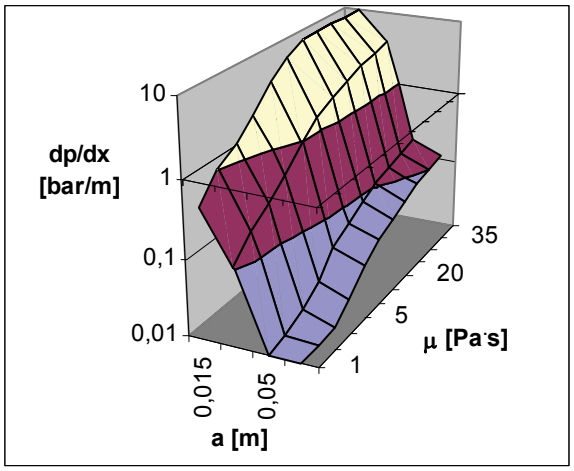

Figure 14: Pressure (dp/dx) vs. radius (a) and plastic viscosity (μ) - no plug (τ_0=5Pa,G_x=1 l/s)

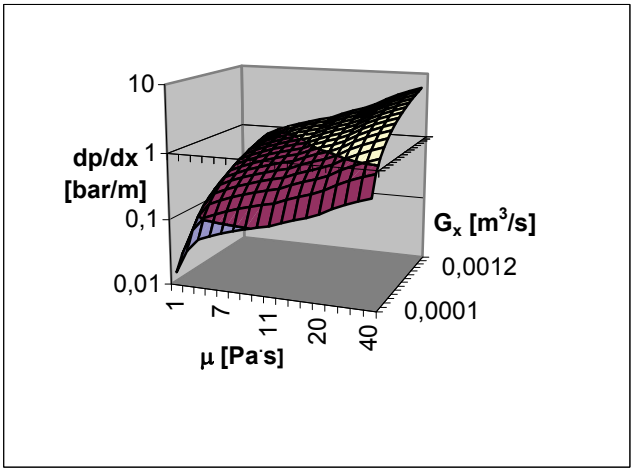

Figure 15: Pressure gradient as function of flow and plastic viscosity (μ) - no plug (a = 0.0225 m, τ_0=5Pa)

Figures 14 and 15 illustrate the very strong effect of pipe diameter, with small pipes giving very high pressure for the range of viscosities of some typical flowing concretes. The effect of plastic viscosity on pressure is also quite strong and the use of logarithmic scales indicates what kind of power law relationships between the main variables we expect to observe in pumping of concrete.

We should also keep in mind that unless the pressure gets too high we can assume that screw pumps (and then also piston pumps since the backflow problem does not exist there) produce quite constant flow. The resulting pressure or –gradient (dp/dx) can be used as parameter for pumpability.

The flow in fig.15 is of course very low for large pipes, but 1 litre/second is realistic for the smaller diameters in figure 14 where there is a very strong effect on concrete pressure of changing the diameter. From figure 15 we also see that the simplification of constant flow is reasonable for our screw pump equipment. A range of concrete qualities tested at 25 Hz frequency had fairly constant flow 0.23 – 0.28 m/s in a = 0.015 m and 0.41 – 0.92 m/s in a = 0.0225 m hoses. The plastic viscosity for these materials varied from < 1 to > 25 Pa·s measured in the co-axial BML-viscosimeter. (Similar plots as those in figures 14 and 15 with yield shear τ_0 instead of μ from our experiments showed very little effect on pressure).

The existence of a plug has been discussed and it has often been argued that, depending on a number of factors, most of the concrete is moving in that fashion (Ede 1957, Johansson&Tuutti 1976, ACI 1998, Kaplan 2001, concrete society 2005, Haist and Muller 2005, Watanabe et al 2007). The plug flow concept is however not univocal since visualization with coloured concrete hardened in pipes have shown flow profiles (Rössig 1974, Kaplan 2001, Kalogiannidis 2008). The consequence of the Bingham model (and any model with a yield shear) is, however, that there will be a gradual transition from plug to shear profile as increasing parts of the fluid in the cross section is brought into shear at increasing flow rate. At the equivalent radius R_0 of a plug in a Bingham fluid, the shear τ acting on the tubular plug wall is equal to the yield shear τ_0, see figure A2 in appendix 1:

$$R_0 = (2L/\Delta p)\bullet\tau_0 \quad (2)$$

Appendix 1 is limited to a solution of the flow of concrete through a pipe based on Hagen Poiselle flow combined with the Bingham material model resulting in the Buckingham-Reiner equation. Figure 16 below shows an example of calculated plug flow (plug radius = 3.8 mm according to eq.(2)) for a concrete pumped through a 45 mm diameter hose based on observed data on rheology and pressure gradient from table 5 (Mork and Jacobsen 2008), see details in appendix 3.

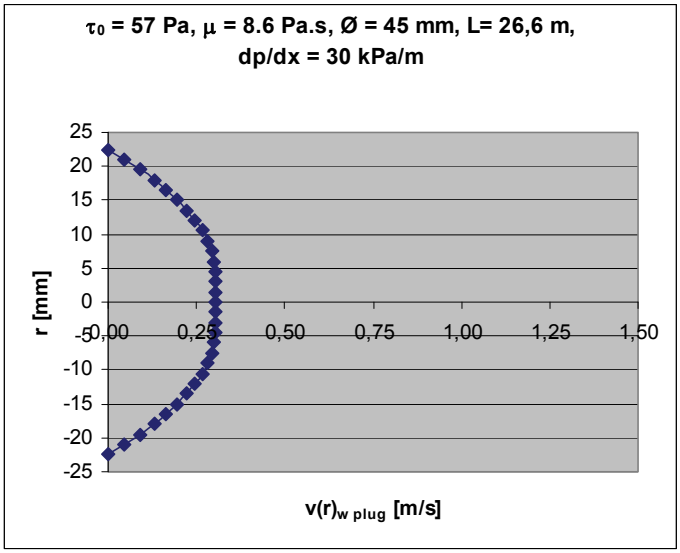

Figure 16: Calculated plug flow profile with measured rheology and pump pressure (appendix 3)

The measured flow of the actual concrete in figure 16 was 0,60 m/s whereas Buckingham Reiner predicts only 0,17 m/s in line with earlier research. The Bingham model was used to describe concrete rheology in pipe flow in (Rössig 1974), but measurements of μ and τ_0 on pumped concrete in a concentric viscosimeter were made for the first time a while later (Hansen 1988, Hu, deLarrard 1996, Kaplan 2001). Pumped high performance concretes with μ in the range 70 – 500 Pa.s and τ_0 in the range 50 – 2000 Pa were studied in the latter two studies. Based on that τ_0 in the actual range has little effect on the last terms within the brackets of the Buckingham – Reiner equation, eq.A9 in appendix 1, the plastic viscosity was expected to be the main parameter affecting pumpability (Hu, deLarrard 1996). Pursuing the effect of viscosity on pumpability, it was found that pumpability relates best to the plastic viscosity in the slip zone ($\mu_{SL\ spec}$ - Pa·s/m) (Kaplan 2001). The slip zone viscosity was calculated from pumping experiments making a number of assumptions. It was also measured with a tribometer developed from the BTRHEOM viscosimeter (deLarrard et al 1993, Kaplan 2001). The slipzone viscosity calculated from pumping trials related well to tribometre experiments on the same concrete. The correlation between the slip zone viscosity and the plastic viscosity of the bulk concrete, measured with the viscosimetre, was however weak. Yield shear in general gave weaker correlation to pumpability in the study (Hu, deLarrard 1996) as opposed to the observations (Hansen 1988). Based on our own results, presented and discussed in section 5, it might at present seem that the plastic viscosity may be a more important parameter than the yield shear stress parameter. It could thus be that the main use of the yield shear stress is to evaluate the degree of plug flow using for example equation (2). Similar tribometers as the one made in (Kaplan 2001) have later been developed and successfully used to quantify power-laws for pumpability through screw pumps (Hellman 2007, Koski 2007).

In Figure 17 the rheological properties of the slip layer around the 3.8 mm radius plug in figure 16 is adjusted into a Bingham material to give the measured flow v_x = 0,60 m/s. This results in a specific plastic viscosity of 131 Pa·s/m of the layer between the plug and the wall, which is in the same range as found in (Kaplan 2001), see details in appendix 4.

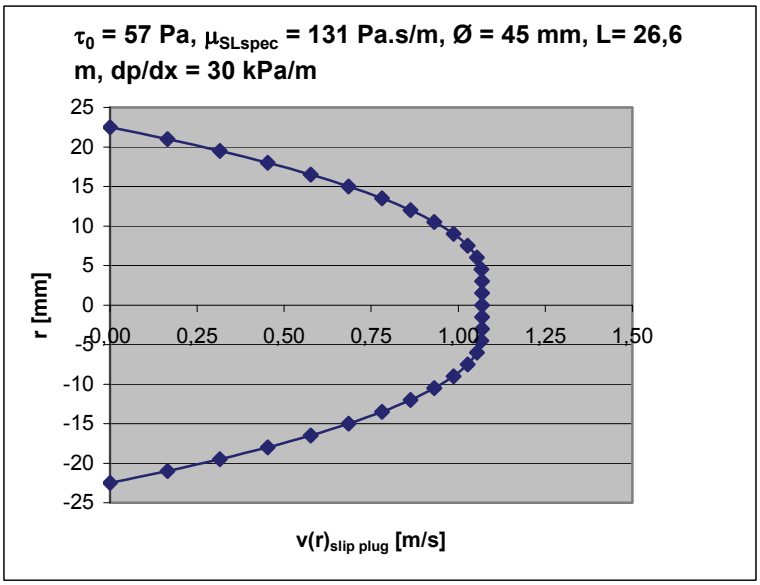

Figure 17. Calculated profile with Bingham properties of slip layer adjusted so that mean flow rate fits the v_x = 0,60 m/s flow measured in the pumping experiments, appendix 4.

Note that if there is a flow profile with or without a plug, it should have developed over some length at some initial flow stage after the pump. This would then lead to some kind of radial in-line mass transfer that could lead to some kind of in line mixing which is not explained or included in the simplified uniaxial flow analysis in Appendices 1, 3 and 4. Kaplan (2001) claimed that there is no radial transfer, whereas Thrane (2007, p.53) seems to be in favour of such radial transfer, at least of coarse particles. Experimentally one should observe a radial pressure gradient to have a radial flow. By looking closely at the longitudinal and transversal pressures in Figure 3 no such signs are seen, but admitting that this does not represent a very detailed study of the existence of radial flow. From experimental observation it seems that coarse aggregate tends to concentrate in the centre of the pipe (Haist and Muller 2005). From a fluid mechanics point of view, it is expected that flow profiles such as in figure 17 would produce lower pressure towards the centre due to the higher flow rate there. This follows from the reduced pressure in stream lines going faster than neighbour lines, viz. Bernoullis equation and stream lines curving over a wing compared to those passing straight under the wing.

Flowable concretes may show considerable deviation from the simple linear Bingham model (Tattersall 1976, Mork 1994, Ferraris, de Larrard and Martys 2001). Examples are concretes containing quite high volumes of fillers/powders and chemical admixtures such as 3rd generation water reducing agents (WRA) and viscosity modifying agents (VMA). The Bingham model:

$$\tau = \tau_0 + \mu \frac{dv}{dr} \qquad (3)$$

τ_0: yield shear strength [Pa]

μ: plastic viscosity [Pa·s]

$\dot{\gamma}, \frac{dv}{dy}, \frac{dv}{dr}$: rate of shear [$s^{-1}$]

may then not be sufficient to describe the rheological behaviour. Rheology may then be better described by other non-newtonian models such as Herschel-Bulkley and power law models (Mork 1994) to describe the dependence of shear stress upon rate of shear:

$$\tau = \tau_0 + K\dot{\gamma}^n \qquad \text{(Herschel-Bulkley)} \qquad (4)$$

$$\tau = K\dot{\gamma}^n \quad \text{or} \quad \eta = K\dot{\gamma}^{n-1} \qquad \text{(power law)} \qquad (5)$$

In the commercial FEM-software COMSOL (www.comsol.com) the pseido-plastic fluid Carreau model is used as default:

$$\eta(\dot{\gamma}) = \eta_\infty + (\eta_0 - \eta_\infty)\left[1 + (\lambda\dot{\gamma})^2\right]^{\frac{(n-1)}{2}} \qquad \text{(Carreau model)} \qquad (6)$$

Where is viscosity, λ is a time constant and n is the power law index (n = 0.01 to fit the Bingham model at high shear rate). These rheological models will of course result in other kinds of velocity distributions compared to Buckingham Reiner, as discussed with the numerical simulations in chapter 6. However, the Carreau model gives similar plastic viscosity as the Bingham model at high rate of shear, presumably beyond the yield shear:

$$\mu(\dot{\gamma}) = \frac{\tau_0}{\dot{\gamma}} + \mu \text{ based on } \tau = \dot{\gamma}\cdot\mu(\dot{\gamma}) = \tau_0 + \dot{\gamma}\cdot\mu \quad \text{(Bingham)} \qquad (7)$$

As seen from equation (7) there will be a convergence problem for a fluid with low rate of shear or at rest applying the Bingham model on this form. Appropriate (convergent) material models for numerical simulation of concrete flow are further discussed in section 6.2.

4 Concrete Composition and pumpability

4.1 General – normal density concrete

It has been stated that most concretes today are pumpable, largely owing to the efficiency of modern two-piston pumps (Smeplass 2008). In view of the earlier mentioned effects of rheology on pumpability and some of our own experiences (Mork and Jacobsen 2008) it is, however, appropriate to discuss concrete composition effects on pumpability.

Proportioning/recommendations (Johansson&Tuutti 1976, ACI 1998, Maage 2003, concrete society 2005) usually focus on the amount of fines, the consistency and the bleeding.
The idea is that too little fines may cause fast bleeding, increased friction and facilitate blocking by some kind of in-line segregation of coarse aggregate particles (Kaplan and deLarrard 2005). Too much fines on the other hand may give a too heavy plastic consistency, thus increasing the pressure at a given flow. Today powder and matrix volume (powder + water+admixture) are considered the best way to proportion and control the consistency of concrete (Smeplass UM4 2004, European SCC guide 2005). It is recommended (Smeplass 2004) that a concrete for ordinary reinforced walls with slump 150 – 200 mm should have its matrix volume increased slightly to be pumpable. For self compacting concrete the matrix volume is already quite high. The pumpability is therefore usually no problem unless there are stability problems causing pressurized bleeding and/or plug formation from forward segregation of coarse aggregate during pumping.

The concrete pumpability, quantified as resulting pressure during pumping and probability of blocking, is improved with increasing amount of fines up to a certain optimum level. After that a further increase of fines usually leads to problems with pressure and blockage (Johansson and Tuutti 1976). The optimum amount of fines depends on a number of factors, but is around 450 kg/m^3 concrete (=cement + fines < 0,25 mm) for 16 mm rounded aggregate and traditional Portland cement concrete (Johansson &Tuutti 1976). Other binders and use of admixtures might change this (Spiratos et al. 2003). As a simplification the aggregate grading is often used as a

main parameter in the proportioning of concrete. Table 1 below is a simplification of the gradation recommended for pumpable concrete.

Table 1 Recommended grading (ACI 1998)

Material diameter (mm)	0.125	0.25	0.5	1	2	4	8	16
Sand (%)	6	18	40	67	85	93	100	100
Total (%) (D_{max}=16mm (min.))*	3	4	12	20	28	37	48	100

*: Natural material, for crushed coarse material the amount of 8-16 should be reduced

There are some recommendations concerning content of different types of fines but so far no composite- or particle-matrix approach has been presented (Smeplass og Mørtsell 2003). The recommendation below (Concrete society 2005) takes into account the effect of maximum aggregate size by reducing amount of cement at increasing aggregate size. Density differences of the materials in table 2 will not be reflected in the volumetric proportioning of concrete. This is a serious drawback of table 2 that may cause large variations in volumetric composition. Clearly a particle-matrix approach is needed. There is however a lack of empirical data on the effect of some pumpability quantity of varying matrix composition and –fractions. Furthermore, pozzolans, filler and cement may have density differences in the order 400 kg/m^3 resulting in significant volumetric variations between the particle and matrix phases. It is therefore at present not possible to make recommendations on pumpability of concrete mixes based on volumetric proportions and matrix content, and more data are needed.

Table 2 Recommended amount of fines (< 0,3, 0,25 and 0,15 mm) (ACI 1998, Concr. Soc. 2005)

Material	Amount/limit/spec.	Source
Fines < 0.3mm	15 – 30 % of aggregate*	ACI 1998
Fines < 0.15mm	5 – 10 % of aggregate*	ACI 1998
* only cement content > 280 kg/m^3 included in fines < 0,15mm		ACI 1998
cem+pozz+filler (D_{max} = 10) < 0.25mm	> 450 kg/m^3 concrete	Con soc 2005
cem+pozz+filler (D_{max} = 20) < 0.25mm	> 420 kg/m^3 concrete	Con soc 2005
cem+pozz+filler (D_{max} = 40) < 0.25mm	> 380 kg/m^3 concrete	Con soc 2005

Admixtures will in general improve the workability and pumpability (ACI 1998). Increasing dosage of water reducing admixtures may reduce the pressure in the pump line compared to reference tests, as observed in full scale tests (Kasami et al 1979, Spiratos et 2003). This is in line with the effect of reduced yield shear stress with addition of super plasticizer (Wallevik 1990, Wallevik 2002). The effect will rest on that bleeding or segregation is not increased to become a problem. For high performance concretes with low w/b, pumpability quantified as pressure, might be worsened even with very high dosages of super plasticizers (Lepage et al 1998). A much higher concrete pressure was observed during pumping of a w/b= 0.30 concrete than in a w/b = 0.38 concrete in the same pump configuration in spite of the former having much higher slump than the latter. The loss of slump due to pumping was higher for the w/b = 0.30 concrete. Air entraining agents work positively by reducing the tendency to aggregate segregation and bleeding.

The effect of pumping on the air content has been investigated and different effects have been reported. Traditional concrete from the 80-ies with 320 kg/m^3 was reported to have increased air void content by pumping (Johansson & Tuutti 1976) whereas reduced air content was reported after pumping of superplasticized high performance concrete (Pleau et al 1998). The latter investigation found that the air void structure may not necessarily be destroyed by the pumping. A large part of the lost air content during pumping consisted of dissolution and/or gashing of the large voids. Therefore the air void spacing factor was not so seriously affected. The coalescence or dissolution of the small voids with highest air pressure in addition to the pumping pressure was found to have less effect on the air void structure. This is probably due to that the number of very small (frost protective) voids was still very high after pumping. In (Kaplan 2001) reduced air void

content was observed after pumping. In (Lepage et al 1998) pumpability and effect of pumping on air void content was investigated on w/b=0.38 and w/b=0.30 concretes with hydroxycarboxylic acid water reducer and fatty acid based air entrainers, the latter concrete also with superplasticizer. Air void structure was not affected by pumping the w/b = 0.38 concrete, whereas the w/b=0.30 concrete had serious damage to its air void system by the pumping. So far it seems that a general conclusion is to use air entrained concrete that can be pumped at as low pressure as possible to avoid damage to the air void system.

Mineral admixtures and/or fines content are mainly used to reduce bleeding, also increasing the matrix volume. Small amounts of silica fume may for example replace a larger quantity of fines and still improve pumpability (Maage 2003). To reduce the pumping pressure and avoid blockage the matrix should, in addition to give as little bleeding and as good slip as possible, have high enough plastic viscosity to slow down the acceleration of coarse aggregate particles from the pump impulse, for example from a piston pump. At the same time the plastic viscosity should be low enough to avoid high pressure gradients. In general more concretes are pumpable than the limitations indicated by the recommended compositions.

4.2 Admixtures for pumped concrete – pumping aids

American Concrete Institute report 212.3R-21 (ACI 2004) defines pumping aids as lubricants and fine fillers used to overcome friction or segregation that cannot be controlled by changes in the concrete mixture proportions. Many pumping aids are thickeners that increase the cohesiveness of concrete.

In Australian Standard (Australian Standard) five categories of thickening admixtures for concrete and mortar are identified:

1. Water-soluble synthetic and natural organic polymers that increase the viscosity of water
2. Organic flocculants
3. Emulsions of various organic materials
4. High-surface-area inorganic materials
5. Finely divided inorganic materials that supplement cement in cement paste-fly ash and various raw or calcined pozzolanic materials, hydrated lime, natural or precipitated calcium carbonates and various rock dusts.

In (Rixom and Mailvaganam 1999) the use of admixtures in pumped concrete was split into three classes dependent on the cement content in the mix:

1. Low < 200 kg/m^3
2. Medium 200-300 kg/m^3
3. High > 300 kg/m^3

Admixtures connected to these three categories are:

1. Water-soluble synthetic and natural organic polymers, organic water-soluble flocculants, emulsions and inorganic materials of high specific surface area.
2. Retarding water reducer and air-entraining agents
3. Dispersing agents as calcium lignosulfonates and sodium salts of hydroxycaboxylic acid.

According to the authors, mixes in both low- and high-cement-content classes are generally more prone to problems concerning pumpability than the medium range. In low-cement-content mixes, poor cohesion results in segregation, and in high-cement-content mixes, thixotropy causes pipeline friction.

The use of admixtures in lightweight concrete is also briefly discussed, with recommendation of using air-entraining agent, superplasticizer or thickener for improved pumpability.

In (Pei, M. et. Al 2000) the use of sodium sulfanilate-phenol-formaldehyde condensate (SSPF) as a superplasticizer was studied and the workability parameters were compared with two conventional superplasticizers, sulfonated naphthalene formaldehyde condensate (SNF) and sulfonated melamine formaldehyde condensate (SMF). The SSPF was reported to be more suitable for pumping concrete and SCC.

4.3 LWA concrete

The pumping of LWA concrete is done on routine basis in Germany and the US (Rössig 1976, ACI 98). Problems with loss of workability, increased pressure in the pipe and even blocking due to too much water being absorbed and/or forced into the porous LWA and loss of connsistency is usually met by pre saturating the LWA (Rössig 1974, ACI 1998). However, successful pumping of LWA concrete with initially dry aggregate has been done for a while in Norway. Flowable and pumpable LWA concrete with w/b in the range 0.38 – 0.47, 450 – 520 kg sement and silica fume, fresh density of 1470 kg/m^3 and LWA with low (0 – 4 % by weight) initial moisture content was reported (Johansen 1991). LWA concretes with composition in this range were pumped successfully horizontally and vertically for 32 m in a 125 mm steel pipe (Johansen 1991). The main technologies were to use sufficient matrix and/or water and water reducers so that the absorption and filling of LWA particles not affected the flow. In addition, superplastizicers, cellulose based stabilizers, air void dampers and polymers were used to increase workability, reduce bleeding while maintaining stability.

One of many objectives of the Lightcon project and previous research projects at SINTEF on LWAC was to develop pumpable LWA concrete with dry LWA. One reason for scepticism towards the use of initially dry LWA in high strength concrete had been unexpectedly low strength. The reason was air bubbles forming at the cement paste-LWA interface, presumably due to powerful absorption into dry LWA-particles (Helland and Maage 1993) and subsequent evacuation of air voids from the LWA as water entered. The investigation also found that the strength loss was reduced by remixing the LWA concrete some 20 minutes after addition of water and initial mixing. The remixing reduced the occurrence of weak bond zones due to air voids at the interface between cement paste and LWA particles. A method for prediction of the amount of water pressed into/absorbed in the LWA during pumping was developed (Smeplass 1998, Eurolightcon 1999) using a pressure cell somewhat similar to the cell for measuring pressurized bleeding (Browne and bamforth 1977). Efforts to reduce the absorption in the LWA by impregnation with various agents were unsuccessful. However, the method seems suitable to determine the amount of water pressed into the LWA during pumping. Based on a review of pumping experiences in Europe (Eurolightcon Pumping 2000, Johansen 1991, Mork and Jacobsen 2008) table 3 below compiles some effects of pumping of expanded clay based LWA concrete on some fresh and hardened properties.

All concretes from (Lightcon 2000) were made with presaturated LWA whereas the last 6 LWA concretes (Johansen 1991, Mork and Jacobsen 2008) were made with initially dry LWA. The main conclusion of the tabulated data is that both initially saturated and initially dry LWA particles can be used for pumpable LWAC. Furthermore, there seems to be no univocal negative effect on compressive strength of pumping and the reduction of consistency and increase of density seems to be moderate. The concrete pressure should, however, be monitored since increasing pressure during pumping could be a sign of problems with increased plastic viscosity due to too much water or matrix being forced into the LWA aggregate. Measurements of density before and after pumping can give indications of such forcing into LWA. Increased density is caused by the volume reduction due to water going into the LWA during pumping. For the above concretes the volume reduction was in the range 5 to 50 litres per m^3 fresh concrete, whereas some materials showed no change or even reduced density. The maximum absorption that can be

tolerated will of course depend on the matrix volume and its rheology. The figures indicate that the surplus of water needed can be relatively large so that there will sometimes be a need for special efforts to reduce instability problems (segregation, bleeding) associated with the high water content. In addition, precaution with respect to excess moisture loss, shrinkage etc. in hardened concrete is needed.

Table 3. Compilation of pre- and post pumping properties of LWA concrete pumped in full scale (EuroLightcon 2000 (EL), Johansen 1991 (J91), Mork and Jacobsen 2008 (MJ))

$f_{c,pre}$ MPa	$f_{c,post}$ MPa	ρ_{pre} kg/m^3	ρ_{post} kg/m^3	$flow_{pre}$ cm	$Flow_{post}$ cm	Data Successful Pumping P: piston, R; screw H: horizontal; V: vertical	Ref
-	22	-	(1650)	75	-	P, Ø125mm, 10m H, 10 m V	EL p.31
30.6	24.6	(1700)	-	-		P	EL p.32
24.3	28.7	1540	1623	50	49	P, 25m H, 10m V	EL p.33
22,2	22	1445	1430	47	45	P, 25m H, 5m V	EL p.34
42.5	49.8	(2000)	-	-	53	P	EL p.35
51.1	55.6	1870	1930	22 (slump)	20 (slump)	P, 250m H, 50m V	EL p.45
-	30	1835	-	16 (slump)	8 (slump)	P, 60 m ?, 4 pumps 75 m^3/h	EL p.49
-	17.5	-	1800	28 (slump)	24 (slump)	P, 30m ?	EL p.51
-	-	-	-	22 (slump)	21 (slump)	P, 154m V, 40 - 60 m^3/h	EL p.54
27.5	26.8	1470	1470	>20(slmp)	>20(slmp)	P, 32 m V	J91
27	31.1	1620	1700	80	71	R, 26,6 m H	
52.7	50.6	1920	1930	73	69	R, 26,6 m H	
27.7	24.7	1670	1660	70	73	R, 26,6 m H	M&J08
52.9	45.6	1890	1820	90	76	R, 26,6 m H	
29.5	28.7	1700	1730	56	54	R, 26,6 m H	

In a publication from the Norwegian concrete association it is recommended that LWA concrete can only be pumped if there is less than 10 % loss of 28 day compressive strength after pumping compared to concrete placed without a pump (Norsk Betongforening 1999). Two of the five LWAs in (Mork and Jacobsen 2008) failed to pass this criterion by comparing strength of specimens made before and after pumping. A closer look at minimum pump pressures and necessary re-mixing required to succeed could be a way of proceeding with this. Perhaps the pressure in the fresh concrete should be measured on routine basis during pumping for certain concretes.

5 Results of instrumented pumping tests in lab and rheology measurements

Some preliminary laboratory pumpability studies were performed with measurements of concrete flow, pressure gradient over the hose and energy consumption in the screw pump. The pump set up consisted of a full-scale dry mix silo, continuous mixer, feeder with additional screw at bottom before and towards inlet of screw pump, and reinforced rubber hose. The complete set-up from maxit Group m-Tec was installed in the NTNU concrete lab as part of the Research Council granted “Skattefunn” project. The set up is instrumented with sensors for concrete pump flow, - energy use and concrete pressure at different stages of the pump/hose system. The sensors are a load cell, an ampère meter and two pressure sensors (Jacobsen and mork NBdag 2007, Mork and Jacobsen 2008). All signals are collected, conditioned, amplified, stored etc in a National Instruments LabView environment.

All preliminary tests referred in this report were run on 12 different mixes previously reported (Mork 2007b, Mork and Jacobsen 2008). These mixes consisted of 4 ND and 4 LWA mortars with total w/c in the range 0,43 – 0,69 and 4 commercial premix products (one LWA concrete, one SCC, one and one screed). The compositions of the 4 ND and 4 LWA mortars are given in (Mork and Jacobsen 2008) whereas product details of the premix products are given in (Mork 2007b, Mork and Jacobsen 2008).

Figure 18 and table 4 show measurements of pressure, energy consumption and flow on a concrete with initially dry LWA. It was found that the screw pump produced quite constant flow, pressure and energy consumption during the 4 consecutive 30 second pumping measurements. As can be seen the age had an influence on the rheology, observed as increased pressure and pumping energy at a quite constant pump flow. The presented measurements were made on a premix LWA concrete with initially dry LWA with pumping and measurements repeated over a 49 minute period.

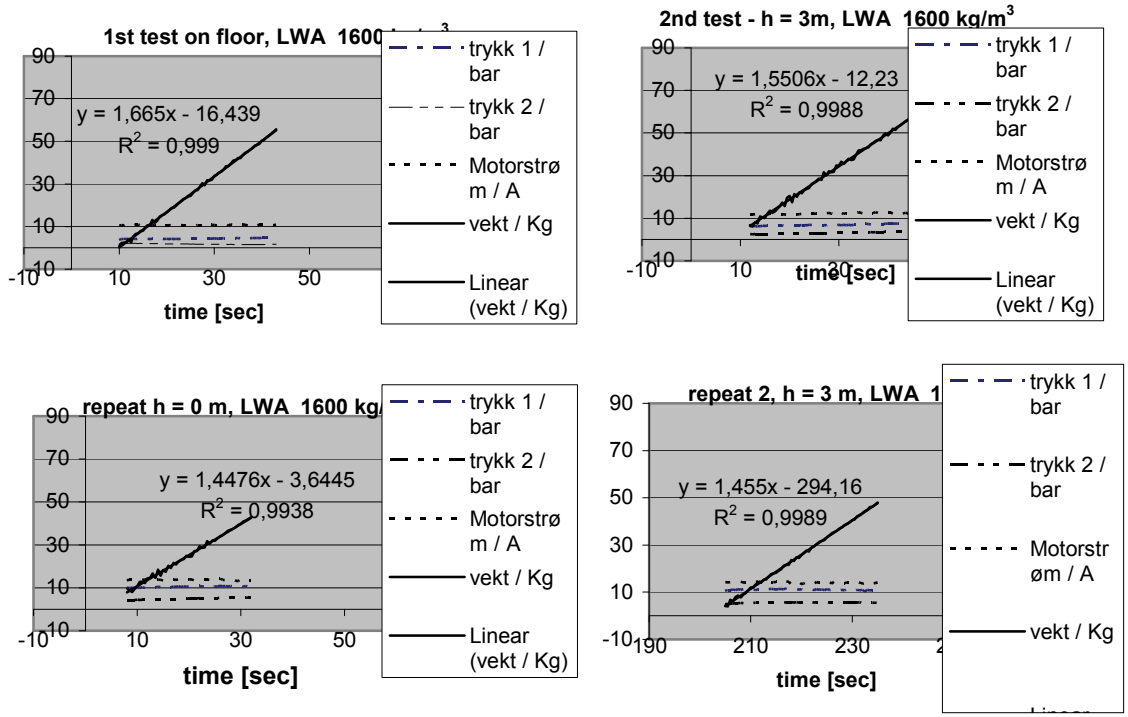

Figure18. Concrete flow, -pressure and electric current during pumping of LWA concrete (1600 kg/m^3) over 49 minutes through 26.6 m Ø 45mm rubber hose at 0 and 3 m height

Table 4. Concrete flow, -pressure and electric current measured in figure 18

Parameters	h = 0m, 1st trial t = 0	h = 3m, 1st trial t = +9 min	h = 0m, 2nd trial t = +44 min	h = 3m, 2nd trial t = +49 min
Concrete flow [m/s] (assuming 1600 kg/m^3)	1,665kg/s (100%) = 0,66 m/s	1,551kg/s (93%) = 0,61m/s	1,448kg/s (87%) = 0,57 m/s	1,455kg/s (87%) = 0,57 m/s
Concrete pressure pump/halfway [bar]	4,4/1,8 (100/41%)	7,1 / 3,3 (100/46%)	10,5/4,9 (100/47%)	11,0/5,6 (100/51%)
El. current [Ampère]	10,7 (100%)	12,2 (114%)	13,7 (128%)	14,1 (132%)

The flow through the screw pump working at constant frequency of 25 Hz (50 % of max capacity) reduced somewhat over the 49 minute period. Two possible causes are; reduced workability with

increasing time and reduced driving pressure difference at 3m height. The hydrostatic component is Δp_{3m} = 1600 kg/m^3*9.81 m/s^2 *3m • 0,5 bar, $\Rightarrow \nabla p_{3m}$ =(dp/dx)$_{3m}$ = 50000 Pa/26,6m = 1880 Pa/m. ($-\frac{1}{\rho}\nabla p + f = 0$, see Appendix 2). This is only around 10 % of the lowest measured pressure gradient in table 4: 4.4 bar/26.6 m = 16500 Pa/m. Since this hydrostatic component only applies in two of the four measurements, ageing is probably the most important cause for increased pressure and reduced flow. The ageing includes normal cement dissolution/coagulation/hydration effects in addition to reduced paste volume and -flow since water is absorbed in LWA. Water absorbed in LWA also increases concrete density, contributing to reduce the volumetric flow even more than the flow based on constant density and gravimetric measurements. The increasing electric current indicates that the required pump energy increases to be able to keep the flow almost constant as concrete pumpability is reduced in line with figure 6 and the observations of increased plastic viscosity etc in (Mork 2007, Mork and Jacobsen 2008).

In addition to studying the pressure, flow and energy consumption, a large number of measurements of properties of fresh concrete were made. At varying stages of the mixing/pumping process measurements were made of pumpability (flow, pressure, energy use) and rheology (Bingham parameters (τ_0 and μ) with BML-viscometer (Jacobsen and Mork 2007, Mork and Jacobsen 2008), slump, flow, T_{50}, density and air void content). The measurements on fresh concrete were made to a maximum age of approximately 45 minutes, depending on how many steps of the pumping process that were investigated (mixing, pumping, pumping through 1 or 2 hoses), and whether batch- or continuous mixer was used.

12 different normal density and lightweight aggregate mortars and concretes were investigated. This included 4 premix materials and 8 ordinary mixes. All materials were mixed for 5 minutes in batches of 150 litres in a counter current horizontally rotating laboratory mixer. The four premix materials were in addition tested in the continuous mixer with only about 20 seconds mixing. After mixing all materials were poured into the pump feeder for pumpability studies combined with rheology measurements.

In spite of some variations in age of fresh concrete at time of measurement, some comparisons could be made to investigate the relation between the pumpability and the rheological properties. This could best be made with measurements made at the same place, which is after pumping through 26,6 m of hose.

The water content of continuously mixed pre-mix mortar was checked with a microwave oven immediately after mixing and the w/c variation of the premix in the continuous mixer was found to vary in the range +/- 0.03. Tests on batch mixes were then made with the same materials at a constant mean w/c.

A large amount of results on rheology and pump flow and pressure were obtained in these initial pump trials. We concentrated on making the rheological measurements as close as possible before and after the measurements of pump flow and energy consumption, and pressure in the hose. However, usually there was a time difference in the order of 10 minutes between rheology- and pumpability measurements. The main effect of pumping on rheology was little change or slightly improved workability measured as slump, T_{500}, flow, τ_0 and μ after pumping compared to after only 20 sec continuous mixing. Over longer time (up to approximately 45 minutes) the pumping process in general seemed to act like some kind of remixing keeping the material workable though stiffening.

For materials with widely varying rheological properties the pump gave approximately constant flow, whereas pressure in the fresh concrete in the hose during pumping varied considerably between the different materials (Mork 2007, Jacobsen and Mork 2007, Mork and Jacobsen 2008).

The largest comparable test series of this kind for the same pump set up was made on the 4 + 4 ND and LWA mortars and the premix LWA concrete (Mork and Jacobsen 2008). These 9 materials all had flowable or close to self compacting consistencies. In the pumping experiments 26.6 m of 45 mm rubber hose was used at 25 Hz pump frequency. The results showed hose flow varying between 0.42 and 0.92 m/s, which is small compared to the variation in plastic viscosity μ and yield shear τ_0. A similar test on 30 mm hose diameter with 6 mixes showed hose flow varying between 0.23 and 0.28 m/s which is even better in terms of low flow variation for materials with varying rheological properties. In table 5 below the main results and rheological data of the concrete after pumping over 26.6 m are tabulated.

Table 5. Rheological data and pumpability measurements of 12 materials pumped at 0,16 – 0,20 lit/s (= 0,23 – 0,28 m/s) in Ø30mm and 0,66 – 1,47 lit/s (0,41 – 0,92 m/s) in Ø45mm simplified analysis of plug flow and turbulence (Jacobsen and Mork 2007, Mork and Jacobsen 2008)

a (radius) m	Material	BML plast.visc. μ Pa.s	Measured over 26,6 m dp Pa	BML yield str τ_o Pa	$(2L/\Delta p)\tau_0$ R_{plug} mm	Meas v_x m/s	Meas G_x lit/s	Re
0,015	EXM m-Tec	16,5	30000	4,4	8	0,28	0,20	1
0,015	EXM batch	14,2	170000	13,3	4	0,27	0,19	1
0,015	JMS m-Tec	25,5	2000000	873	23	0,25	0,18	1
0,015	JMS batch	23,1	2000000	875	23	0,23	0,16	1
0,015	REP m-Tec	21,4	100000	130	69	0,25	0,18	1
0,015	REP batch	7,4	10000	55	293	0,25	0,18	2
0,0225	Reference 4mm 30 MPa	3,7	735000	146,05	11	0,42	0,67	10
0,0225	Reference 4mm 60 MPa	5,78	726000	144,81	11	0,66	1,05	10
0,0225	Reference 8mm 30 MPa	2,05	476000	61,42	7	0,71	1,13	31
0,0225	Reference 8mm 60 MPa	8,57	797000	57,05	4	0,60	0,95	6
0,0225	LWA 4mm 30 MPa	4,6	332000	228,49	37	0,89	1,42	14
0,0225	LWA 4mm 60 MPa	2,7	489000	82,74	9	0,41	0,66	11
0,0225	LWA 8mm 30 MPa	1,33	283000	21,82	4	0,64	1,01	34
0,0225	LWA 8mm 60 MPa	0,98	293000	5,59	1	0,92	1,47	68
0,0225	maxit ton 915 m-tec	2,66	529000	96,19	10	0,64	1,01	17

In the tests presented in table 5 all kinds of consistencies of the material coming out of the hose end were observed from apparent plug flow, to highly flowing self compacting materials. Following the above discussions on the low variation of pump flow we have plotted pressure as function of the two Bingham parameters in figures 19 and 20 below.

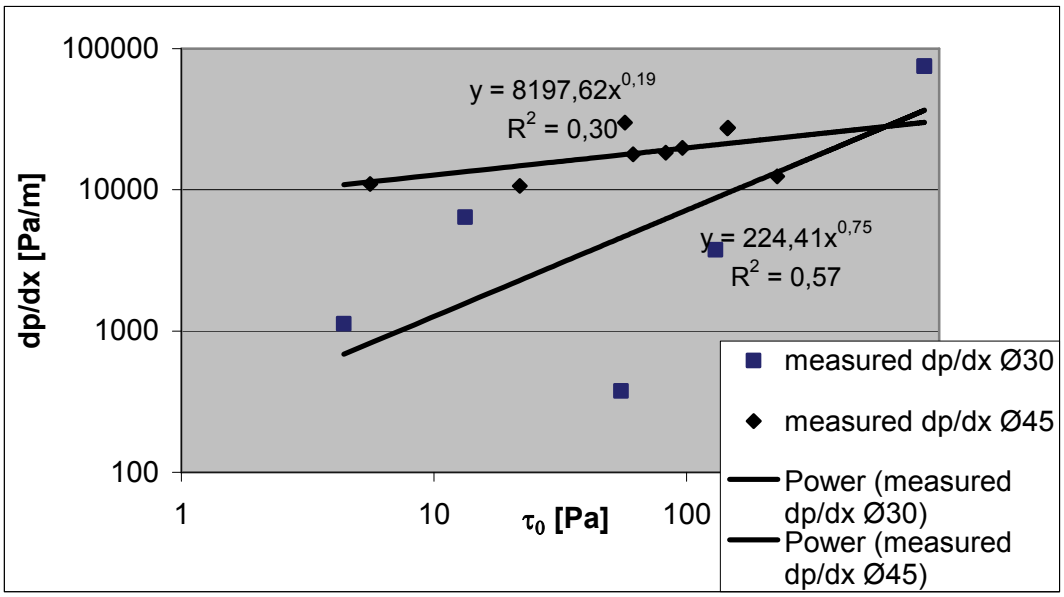

Figure 19. Relation dp/dx vs yield shear (τ_0) at approximately constant flow 0,16 – 0,20 lit/s (= 0,23 – 0,28 m/s) in Ø30mm and 0,66 – 1,47 lit/s (0,41 – 0,92 m/s) in Ø45mm hoses

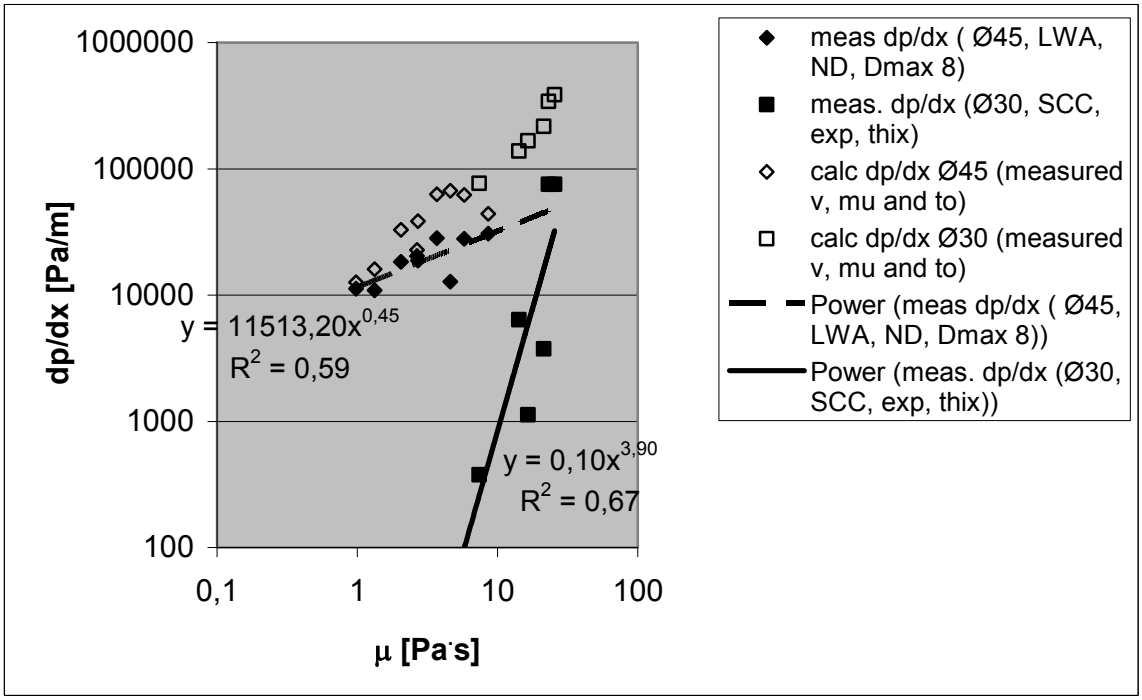

Figure 20. Relation dp/dx vs plastic viscosity (μ) at approximately constant flow 0,16 – 0,20 lit/s (= 0,23 – 0,28 m/s) in Ø30mm and 0,66 – 1,47 lit/s (0,41 – 0,92 m/s) in Ø45mm.

The plots in figures 19 and 20 indicate that pumpability quantified as pressure gradient relates better to plastic viscosity than to yield stress. Figure 20 also shows that equation (1) predicts too high pressure for the measured values of flow, plastic viscosity and yield stress. The deviation seems to be larger the smaller the hose radius and the larger the plastic viscosity. The results are in line with earlier findings that Buckingham Reiner predicts too low flow (Hu, de Larrard 1996, Kaplan 2001). Furthermore, the flow was most sensitive to variations of μ within the observed range of values of τ_0, μ and dp/dx. One probable reason for the weakness of Buckingham Reiner is that the plug size and -shape and also probably the rheological properties of the slip layer are unknown. Clearly more experiments and data on the properties of the flow profile are needed.

A simplified analysis of the degree of plug- or laminar/profile flow can be made based on equation (2), pressure measurements in pumping experiments and measurements of τ_0. In fact, the flow of concrete through a pipe can itself be used as a viscosimeter measuring plastic viscosity μ and yield shear τ_0 provided enough information is at hand; pressure difference, flow and flow profile (Hans 2003, Wiklund 2007). Our simplified analysis of the degree of plug flow according to equation (2) and appendix 1 presented in table 5 shows that we have all kinds of variations from plug flow to highly developed flow profiles. In most cases the plug radius is lower than the pipe radius indicating that there is some degree of flow profile. Visual observations were made of the surfaces of the stiff plug materials coming out of the hose. The surface of the dispatched "plug" seemed wetter than the bulk. However, they appeared to dry up or reabsorb the surface water quickly. Sawing of one hardened plug revealed even distribution of aggregate.

An evaluation of the flow profile can also be made with the Reynolds number (Re) to get an idea whether the profile is laminar or perhaps turbulent if Re >> 1:

$$\mathrm{Re} = \frac{v_x d\rho}{\mu} \qquad (8)$$

Here d is a characteristic size, in this case pipe diameter [m]. For Bingham materials we take the plastic viscosity, μ, as a conservative estimate of the Newtonian viscosity (Thrane 2007). As seen from table 5, Re is in the range 1 – 2 for the 30 mm diameter hose. This indicates laminar flow and thus plug flow seems reasonable. However for the 45mm diameter hose, Re is in the range 6 – 68 indicating more viscous or liquid like behaviour and less probability at least for pure plug flow for the concretes tested in this hose. We also note that the materials tested for pumpability in the Ø45mm hose were more flowable than the Ø30mm materials as judged from their lower plastic viscosities. More direct quantitative use of the Reynolds number seems difficult since most experience stems from fluids with viscosity orders of magnitude lower than our materials (Helland 1982, Welty et al 2001).

Finally it should be mentioned that the ACI method in figure 8 to determine pressure for a given pump capacity, set up, pipe length etc with concrete slump as the only rheology parameter, is too rough. For our experiments many concretes with slump in the range 200 mm had much lower pressure than the 17 bar predicted by the use of figure 8 for 8 inch slump and the specifics of our pump-set up. There seems thus to be a need for more work on models and experiments for concrete pressure as function of workability for example for SCC which has much more fluid consistency than the workability range of figures 7 and 8 (Rodum, Hammer 2008). In addition the diagrams cannot predict the effect on pumpability of changing pipe-cross section, which is a matter of practical concern (Smeplass 2008).

6 Calculated flow profiles based on measurements

6.1 Plug flow and slip layer modelling – equivalent visco thickness

In (Ede 1957) friction between concrete and pipe depending on the concrete pressure on the pipe wall was used to calculate resistance to flow. In (Thrane 2007 p.65) a rheological approach was taken considering the concrete as a bingham material with three possible boundary conditions identified for modelling of flow of SCC. These were; no slip and constant μ, slip with constant flow at the wall and constant μ, and a lubrication model with low μ at/near the wall and then a bulk μ for most of the flow a bit away from the wall. A low-viscous slip layer surrounding a stiffer plug is, as shown in section 3.2, one way of solving the problem with the too low flow predicted by the Buckingham Reiner equation. We therefore proceed with a simplified analysis of the degree of plug flow based on table 5 above and the discussion in chapters 4 and 5. As

explained in section 3.2 and appendix 2, the Buckingham Reiner type plug flow can be modified with a surrounding Bingham slip layer as illustrated by fitting the plug flow in figures 16 and 17 to measured flow. This approach may be further developed assuming a no slip boundary were the velocity of the plug is varied by adjusting the rheology and thickness of the slip- or lubricating layer. We still require that the total integrated flow in eq.(A8) in Appendix 1 is equal to the measured flow, and then adapt the plastic viscosity of the Bingham slip layer. In the figures above we used the plug radius based on the shear acting on the concrete near the pipe wall, i.e the plug radius calculated from eq (2) and Appendix 1. In figure 21 below we try a larger and perhaps more realistic plug radius surrounded by a slip layer of only 2.1 mm thickness. Furthermore we assume that both yield shear and plastic viscosity of the slip layer are low compared to the Bingham parameters of the plug material, i.e. some kind of viscous paste or grout lubricating the layer between the plug and the pipe. The detailed calculations are given in a worksheet in appendix 3 and 4.

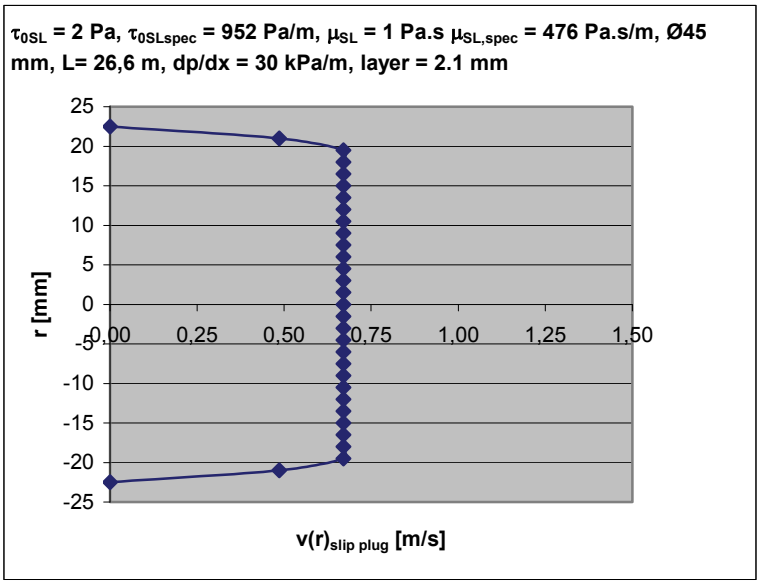

Figure 21. Flow profile with v_x = 0,60 m/s and very viscous 2.1 mm Bingham slip layer (app.4)

In fact we could let the plug radius and rheological properties of the slip layer vary within any combination of layer thickness and layer plastic viscosity with total flow fitted to the observed flow of the pumping experiment. This was done for the above example by integrating the flow profile numerically in 1.5 mm layer steps. Figure 22 below shows a plot of specific plastic viscosity of the (fictive) slip layer vs layer thickness for a constant yield shear (Appendix 4).

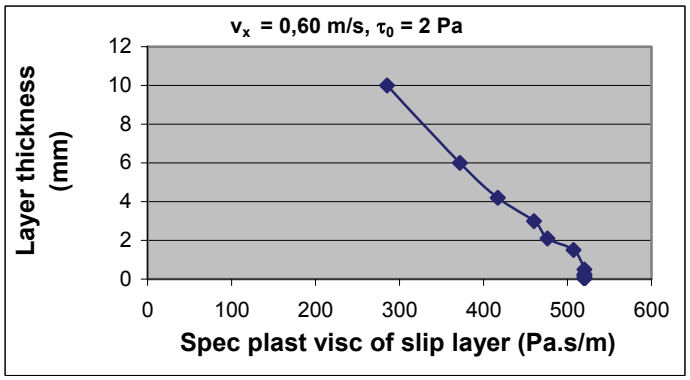

Figure 22. Specific plastic viscosity of slip layer vs layer thickness for plug in figure 21 (app.4)

The relation slip layer viscosity - layer thickness in figure 22 is limited by the coarse integration steps at the surface (1.5 mm). Presumably the specific viscosity of the slip layer will increase towards infinity as the layer thickness is reduced towards zero. However, at present the most

important work lacking is on observing the actual slip layer; both its thickness and its rheological properties. From figure 22 it seems dubious to apply the concept specific plastic viscosity of slip layer when it in the present model actually varies depending on the layer thickness, and presumably also on flow rate.

In order to describe the slip layer properties it could perhaps be possible to use the apparent linear part of figure 22 resulting in a slip layer equivalent visco-thickness coefficient equal to the absolute value of the ratio $d(a-R_0)/d(\mu_{SLspec})$. Figure 22 above gives:

$$d(a-R_0)/d(\mu_{SLspec}) = ABS((10-1.5)*10^{-3}\ m/(285-507)\ Pa\cdot s/m) = 3.8 * 10^{-5}\ m^2/(Pa\cdot s) \quad (9)$$

The proposed visco-thickness can be calculated from plots like figure 22 for all materials in this study to characterize the slip layer. The advantage of such analyses is that the necessary experimental data can be measured in the existing viscosimeter instead of having to use the kind of specially designed tribometer developed in (Kaplan 2001). If tribometres are to be used it would be better to develop an apparatus operating under pressure, perhaps where the pipe material (steel, rubber, plastic etc) can be tested, in addition to measuring the plastic viscosity and yield shear of the slip layer. However, the main objectives of testing and computations are to predict whether the pumping will be successful, and to predict the flow behaviour during the casting process. That is, the whole process from mixing to form filling including pumping should be predictable. Therefore, variations in flow due to differences between pipe- and form surface should not be size dependant so that the same surface should give predictable flow whether in a small or big pipe or in a wide or slender mould with little or much reinforcement. Such an experimental verification or check requires an extension of the flow simulations presented in the next section of this report into realistic 3D models including the casting process and additional experiments following the pumping studies. We therefore recommend that any model for flow of concrete during pumping also should be verified in full scale moulding into varying forms.

6.2 Numerical simulation of flow of pumped concrete

We have chosen to investigate the applicability of an existing commercial software, COMSOL, for simulation of flow of fresh concrete. Aware of other flow models such as the numerical model of flow in the coaxial viscosimetre (Wallevik 2003) and other works on concrete flow such as (Thrane 2007, Roussel 2007) we chose COMSOL for its availability and low user threshold. The generalised Navier-Stokes equation for steady-state flow may be written:

$$\rho\frac{\partial v}{\partial t} - \nabla\cdot\eta(\nabla v + (\nabla v)^T) + \rho v\cdot\nabla v + \nabla p = F \quad (10)$$

and for steady state-flow

$$\nabla\cdot v = 0 \quad (11)$$

where v is the velocity vector (m/s), the density (kg/m^3), η the dynamic viscosity (Pa·s), p the pressure vector (Pa) and F is a volume force field (N/m^3) such as gravity so that $f = F/\rho$ (m/s^2). The equation is explained a bit more in Appendix 2.

Various rheological models, such as the Bingham model, Power-law model, Herschel-Bulkley- and Carreau model, can be related to the Generalized Navier-Stokes equation by establishing the relationship between the plastic or dynamic viscosity (μ, η) and rheological parameters, see section 3.2. Incorporating such models into Navier Stokes equation makes it practically

impossible to solve the resulting differential equations analytically for flow as function of time and space for given boundary conditions, pressure and fluid material parameters.

The FEM-based Comsol Multiphysics Fluid dynamics module is a rather user friendly program solving equation (10). We have here for simplicity made some simulations with Bingham-type fluids in 2 dimensional openings with the same width and length as the diameter and length of the 30 and 45 mm hoses in the experiments. As boundary condition we used only "no slip" which can be seen in all results as zero flow at the wall. Furthermore we used only a simple 2D representation of the pipe in the form of two parallel border lines with width = 45 and 30 mm and length = 26.6m.

Concrete in its fresh state may be considered to behave like a viscoplastic fluid with the rheology of normal fresh concrete described by the Bingham model or Hershel-Bulkley model as mentioned already in section 3.2, see also Appendix 1. However, both models, see eq.(3), (7) and (4) respectively, have problems with convergence at low or zero strain rate when simulations based on them are run in COMSOL Multiphysics. To overcome the convergence problem the Bingham model was modified by introducing a term of $(1-e^{-m\dot{\gamma}})$ with the constant m • 100, to the constitutive equation as below (Papanastasiou 1987):

$$\eta(\dot{\gamma}) = \frac{\tau_0}{\dot{\gamma}}(1-e^{-m\dot{\gamma}}) + \mu \qquad (12)$$

In this way problems with low or zero rate of shear is avoided. Simulations based on the Papanastasiou Model (user defined model) and the Carreau Model (default model of Comsol – see eq.(6)) were run in COMSOL Multiphysics by using the rheological parameters shown in Table 5. The results are given in table 6, examples of flow profiles are shown in figures 23 and 24. In Appendix 5 all flow profiles are shown.

Running simulations by the Carreau model are mainly based on the approach that at high strain rates and $_{o}$ » ., the Carreau model becomes the Bingham model. This approach works well on the shear region but not on the plug region in the flow. If the shear region in the flow involves high strain rate, then the simulation results obtained in this region will be closer to the reality. Therefore the velocity profiles obtained by the Carreau model are not so perfect when compared to those by the Papanastasiou model. Although the Papanastasiou model, which is the modified Bingham model, can give a better velocity profile, it takes much longer to converge to a solution of equal accuracy as the Carreau model. However, from figures 23 and 24 shown below, the flow velocity by the Papanastasiou model is lower than that by the Carreau model.

From the comparison of velocity profiles obtained from both models, clear plug flows can be seen for most cases when using the Papanastasiou Model, see Appendix 5. The radii of the plugs can be estimated from the velocity profiles and compared with the calculated values using the Buckingham Reiner equation. In table 6 below we have collected measured flow together with calculated flow using the analytical solution (Buckingham reiner) as well as the numerical solution with Navier stokes equation and the Papanastasiou model.

Table 6: Measured and calculated (analytical, numerical) solutions

a (radius) m		Measured v_x m/s	Calc Buck-R v_x m/s	Calc FEM 2D v_x m/s	Plug radius R_0 estimate FEM 2D
0,015	EXM m-Tec	0,28	0,00	0,00316	4 mm
0,015	EXM batch	0,27	0,01	0,0266	3 mm
0,015	JMS m-Tec	0,25	0,07	0,0156	12 mm
0,015	JMS batch	0,23	0,08	0,0169	12 mm
0,015	REP m-Tec	0,25	0,72	$5{,}24*10^{-6}$	0
0,015	REP batch	0,25	0,00	$1{,}06*10^{-6}$	0
0,0225	Ref 4mm 30 MPa	0,42	0,18	0,8203	6 mm
0,0225	Ref 4mm 60 MPa	0,66	0,12	0,5176	7 mm
0,0225	Ref 8mm 30 MPa	0,71	0,33	1,1340	5 mm
0,0225	Ref 8mm 60 MPa	0,60	0,60	0,5127	3 mm
0,0225	LWA 4mm 30 MPa	0,89	0,20	0,0223	20 mm
0,0225	LWA 4mm 60 MPa	0,41	0,20	0,8049	5 mm
0,0225	LWA 8mm 30 MPa	0,64	0,38	1,1616	3 mm
0,0225	LWA 8mm 60 MPa	0,92	0,67	1,8640	1 mm
0,0225	Maxit ton 915 m-tec	0,64	0,21	0,8569	6 mm

From table 6 and Appendix 5 the main conclusions are that convergent numerical solutions for Bingham materials are obtained and with similar plug shaped velocity profiles as in the analytical solutions. Furthermore it seems that the numerical simulations are closer to the measured flow for the larger pipe diameter. By comparing with the analytical plug-radii of table 5 we see that the numerical model seems to predict somewhat smaller plug radii. However, since the geometry differs between the two models we do not expect any match between simulations and analytical solutions. (The simplified geometry in the FEM model should make its flow less influenced by the slip conditions the larger the width since the ratio (Flow Area/Aspect) for a slit approaches 0.5 at increasing width. For a circular pipe the same ratio is monotonically increasing with increasing diameter as half the radius; r/2. Therefore we would also expect smaller plugs for the slit geometry than for the tube geometry).

Further investigations should aim at making a rotational symmetric numerical model that can be solved with reasonable computer power where different slip conditions are studied and compared with experiments. The experiments should aim at studying the basic rheological parameters expected to affect pumpability as well as some pipe and pump characteristics. Rheology, pumpability and flow profiles of matrix and concrete with varying plastic viscosity and yield strength should be investigated as function of pump frequency and pipe materials. Later the pressure conditions in larger pipes and piston pumps should be investigated, and the flow during form filling should also be checked. Also non-bingham behaviour such as shear thinning and thixotropy should be investigated (Wallevik 2003, Roussel 2007) to find possible effects on pumpability.

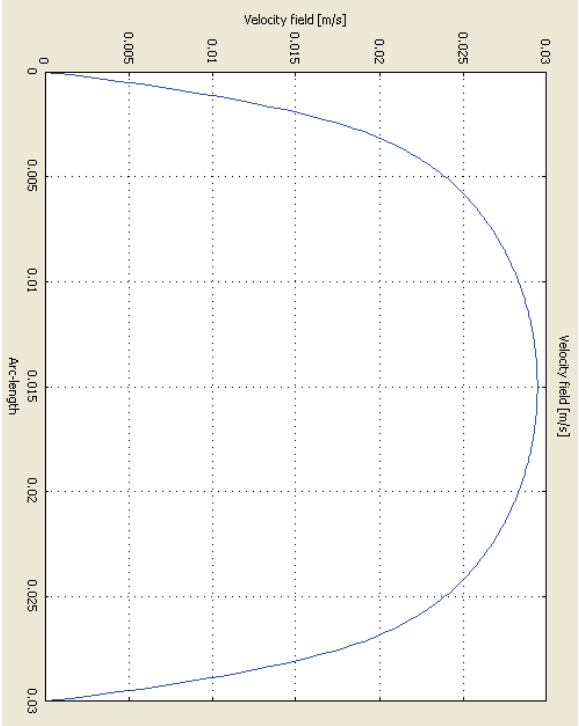

Fig. 23. JMS M-Tec, by Carreau Model

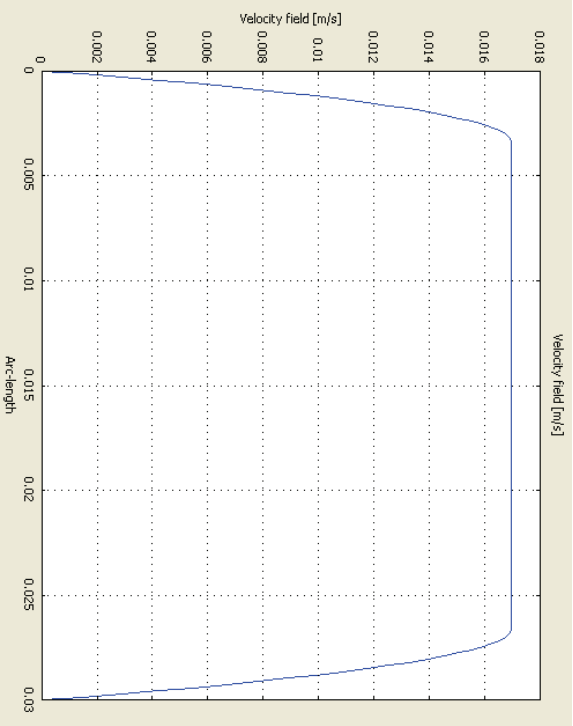

Fig. 24. JMS M-Tec, by Papanastasiou Model

7 Conclusions

The pumpability of concrete, or its ability to move through pipes and hoses by the help of a pump, while maintaining its fresh and hardened properties, can be quantified as being better the lower the necessary pressure to obtain a given flow in a specific configuration (pump type, -capacity, pipes/hoses, diameter, length etc). A range of properties can be specified to define pumpability including the effect pumping has on hardened properties.

The practical pumping process including the principles of piston- and screw pumps show that for a wide range of concretes the flow in a given set-up is approximately proportional to pump-frequency whereas resulting pressure depends in addition on concrete technological parameters (concrete composition, rheology). Based on review and some preliminary pumping trials in our lab we propose concrete pressure gradient over the line as a measure of pumpability for a given pump set-up.

The traditional pumpability criteria based on sufficient slump and low rate of bleeding still yield, and a new simple method measuring pressurized bleeding in the conventional air void apparatus is a simple and inexpensive test that can be used on site on 5 litre samples with air pressure. 20 cm^3/hour bleeding is proposed as maximum rate of bleeding during the first 60 minutes in this simple pumpability test.

Existing recommendations on composition of pumpable concretes are inadequate since they are mainly based on mass or -percentage of various binder and filler fractions without consideration of volumetric variations that may arise from density differences. Consequently the basis for proportioning concrete is violated. Clearly a test programme with rigorous proportioning based on particle – matrix approach including adequate correction for measured air void content and measured density combined with the criteria of ACI and Concrete Society and full scale pumpability tests should be conducted to verify criteria for more flowable concretes than those in present guidelines. So called pumping aids are usually divided into organic and inorganic

materials including thickeners and inorganic powders, where improvement of stability against separation is one important effect of these.

We present some results on flow calculations and pumping experiments on mortar and concrete mixes; both commercial premix products and open lab mixes. Measurements of rheological parameters in the BML-viscometer and pressure, concrete flow and energy in an instrumented full-scale pump-set up with a screw pump, indicate that plastic viscosity is the main rheological parameter affecting pumpability. This includes LWA concrete, but there special considerations must be taken to ensure sufficient matrix volume to secure the plastic viscosity in case pumping pressure gives volume reduction and loss of pump flow due to too much water going into the LWA. Also possible negative effects on strength must be controlled according to existing LWA recommendations.

Finally we analyse the degree of plug flow and find that within our tests there are probably a wide variety of flow profiles from plug to near-turbulence. Analytically calculated flow in pipe is lower than measured flow, probably more so the higher the degree of plug flow. Numerical simulations were made for a simplified 2D case solving Navier Stokes equation using a commercial FEM software with a convergent solution of the Bingham model. The numerical simulations gave similar plug flow as the analytical solutions.

Continued research on the pumping process should study flow characteristics like velocity profile, plug, slip layer properties and concrete rheology effects (admixtures, matrix volume and – properties) on pumpability. Studies of pump frequency, increasing vs decreasing flow, hose characteristics (material, diameter, length, height etc) on concrete pressure, flow profile and slip layer should be carried out. In addition numerical models should be developed and various practical cases should be verified such as form filling, effect of pipe material and dimensional changes. Any discrepancies between reality and numerical predictions using Navier Stokes equation should be further investigated to give generalized solutions for both pumping and casting.

8 Acknowledgement

The work is part of an ongoing research project in collaboration between maxit Group and The Norwegian University of Science and Technology (NTNU), Department of structural engineering and supported by the Research Council of Norway as well as the concrete innovation centre (COIN) where maxit Group and NTNU Dept of Structural Engineering are two of the partners.

The experiments described were carried out in the concrete laboratories at NTNU dept of structural engineering but due to their labour intensive nature would not have been possible without assistance from colleagues and partners at NTNU, maxit Group and SINTEF; Laboratory engineer Ove Loraas, Andreas Gurk, Jon Elvar Wallevik, Göran Lorås, Geir Norden, Mårten Ekelyn, Bruno Jensen (maxit Group), in addition to help and support from Dr Hedda Vikan and Dr Tor Arne Hammer, task responsible of COIN/TG 2 at Sintef and COIN centre leader, respectively.

9 References

ACI Comm. 304 (1998) Placing concrete by pumping methods, ACI 304.2R-96, 2nd Print 25 p.
American Concrete Institute (ACI) (2004) rep. 212.3R-04, Chem. Admixtures for Concrete, 30 p.
Australian Standards MP 20.2, Thickening Admixtures for Use in Concrete and Mortar
Bartos P.J.M., Sonebi M., Tamimi, A.K.(2002) Workability and rheology of fresh concrete: compendium of tests, Report of Rilem TC 145-WSM, Workability of special concrete mixtures, ISBN 2-912143-32-2, 127 p.
Browne Roger.D, Bamforth Phillip B. (1977) Tests to establish concrete pumpability, ACI Journal May 1977, 193-203
Concrete Society (2005) Pumping concrete, Good Concrete Guide 2, Surrey, 14 p.
De Larrard F., Szitkar J.C., Joly M., Claux F. and Sedran T. (1993) Design of a rheometer for fluid concretes, RILEM Workshop, Ed.: P.Bartos, E&FN Spon 201-208
DeSchutter (2007) December 4, personal communication
Ede A.N.(1957) The resistance of concrete pumped through pipelines, Magazine of Concrete Research, November, 129-140
EuroLightcon (1999) Methods for testing fresh LightWeight Aggregate Concrete, Document BE96-3942/R11, 51 p.
EuroLightcon (2000) Pumping of Light weight Concrete based on expanded clay in Europe, Document BE96-3942/R11, 65 p.
European guidelines for Self compacting concrete (2005) Specification, production and use. ERMCO/CEMBUREAU/EFNARC, 63 p.
Ferraris C., de Larrard F, Martys N.(2001) Fresh Concrete Rheology : Recent developments, in Materials Science of Concrete VI, Amer. Cer. Soc. Ed.S.Mindess, J.Skalny 215-241
Feys, D, Calie B., Verhoeven R., De Schutter G.(2007) Evaluation of gravitational flow tests with SCC in pipes as a forecast for pumping pressures, 5th Int. symp. on SCC, Rilem PRO54 ISBN 978-2-35158-047-9, Vol.1, 515-520
Haist M., Müller H.S.(2005) Optimization of the pumpability of self-compacting Light Weight Concrete, Proc SCC 2005 ACBM, NWU, Evanston, 6 p.
Hansen J.K.B.(1988) Characterisation of concrete pumpability using the two-point apparatus, High Performance Concrete Materials Development report 3.2, report no Sintef STF 65 F89046, Norway, 45 p.
Hans A.(2003) Entwicklung eines In-line viskosimeters auf basis eines magnetisch-induktiven Durchflussmessers, Dr.diss. Schriftenreie Institut fur Mess- und Regelungstechnik, Universität Karlsruhe TH (No.001),105 p.
Helland K.(1982) Fluidmekanikk 3.opplag, Tapir, Trondheim, 151 p.
Helland S, Maage M.(1993) Strength loss in un-remixed LWA Concrete, Utilization of High Strength Concrete, Symp. Lillehammer Norway june 20-23 Proceedings vol 2 Ed. I.Holand, E.Sellevold ISBN 82-91341-00-1, Norw Concrete Association Oslo, 744-751
Hellman F.(2007) Comparison of the power law pressure drop modell versus actual pressure drop in the Vingåker laboratory pump rig, Cementa Res. / Maxit Rep. 68105-08G 11 p.+ 2 app
Hu, C, De Larrard F., Sedran T.(1996) A new rheometer for high performance concrete, 4th Int Symp on High Strength/High performance concrete, Presses de LCPC, 179-186
Jacobsen S., Mork J.H.(2007) Pumping of concrete and mortar, Norwegian Concrete day, SINTEF, 18 p.
Johansen Kjetil (1991) Pumping of LWA concrete with density 1450 (In Norwegian), Norwegian Concrete day, 15 p.
Johansson A, Tuutti, K.(1976) Pumpbetong och betongpumpning (Del 1), Betongmassas strömning i rör (Del 2), CBI rapport 7:76, Stockholm, 10 p.
Jolin M., Chapdelaine F., Burns D., Gagnon F., Baupré D.(2006) Pumping concrete; a fundamental and practical approach, presentation Shotcrete for underground support X, Sept.12-16 (2006) 9 p.

Kalogiannidis E. (2008) Coloured mortar and flow profiles, NTNU/Dept of structural engineering, Sintef, preliminary report, Norway, 27 p.
Kaplan D.(2001) Pompage des bétons, Thèse de doctorat ENPC/ LCPC, ISBN 2-7208-2010-5, Paris, 228 p.
Kaplan D, deLarrard, F., Sedran T.(2005) Avoidance of Blockages in Concrete Pumping Process, ACI Materials Journal, 102 (3) 183-191
Kasami H., Ikeda T. and Yamane S (1979) On Workability and pumpability of superplasticized concrete, Proc. 1st CANMET/ACI Conf on Superplasticizers in Concrete, Ottawa, V.M.Malhotra Ed., ACI SP62, 67-86
Koski Piiparinen, P.(2007) Pumping trials on premix concrete products and the use of the viskomat to evaluate pumpability, Cementa Research / Maxit Report 68105-08J, 14 p.+2 app
Lepage S., Baalbaki M., Lessard M. and Aitcin P.C.(1998) Pumping air-entrained high performance concreteProc Int symp. High-performance and reactive powder concretes Vol.4, Univ.Sherbrooke, 393-404
Lu, Laijun.(2005) Construction Technology of Self-Compacting Concrete, Proc 1st Int Symp on design, performance and use of SCC, SCC'2005 – China, Yu, Shi, Khayat and Xie (Eds) RILEM PRO 042 ISBN: 2-912143-61-6, 617-625
Maage M.(2003) Concrete for various applications, Chap. 1 in Course on Concrete Technology, NTNU, Dept Structural Engineering, 76 p.
Mork J.H.(1994) Effekt av sementens forhold mellom gips og hemihydrat på den ferske betongens reologi dr.ing avhandling 1994:04, NTH, 286 p.
Mork J.H (2007a) Module on fresh concrete,Course Concrete Tecnology 3 NTNU Dept of Struct Engineering 39 p.
Mork J.H.(2007b) More efficient use of mortar on the building site. Pumping and rheology, Maxit Group/NTNU Draft report April 23, 9 p.
Mork J.H., Jacobsen S. (2008) More efficient use of mortar at the building site. Pumping and rheology Pumping and rheological properties of LWA concrete, Maxit Group/NTNU Dept of Structural Engineering/COIN TG2, 23 s.
Norsk Betongforening (1999) publikasjon 22, Lettbetong Spesifikasjoner og produksjonsveiledning, NB Oslo 70 s.
Norsk Betongforening (2007) publikasjon 29, Spesifikasjon og produksjonsveiledning for selvkomprimerende betong, NB, Oslo 48 s.
Papanastasiou, T.C.(1987) Flows of Materials with Yield, Journal of Rheology, 31(5)385-404
Pei, M., Wang, D., Hu X. and Xu D. (2000), Synthesis of sodium sulfanilate-phenol-formaldehyde condensate and its application as a superplasticizer in concrete
Pleau R., Boulet D., Aïtcin, P.C.(1998) Influence of pumping on the air-void system of HPC, Proc Consec '98, Gjørv, Sakai, Banthia (Eds.) E&FN Spon, 2047-2056
Rixom, R. and Mailvaganam, N. (1999), Chemical Admixtures for Concrete, 3rd edition, E & FN Spoon, London, pp. 297-299
Rodum E., Hammer T.A., Jacobsen S. (2008), Veiledning for pumping av betong, SINTEF Byggforsk Betong Rapp.utk 15.jan, 3D0005.02, 17 s.
Roussel N. (2007) Rheology of fresh concrete: from measurements to predictions of casting processes, Materials and Structures (49) 1001-1012
Rössig M.(1974) Fördern von Frischbeton, insbesondere von Leichtbeton, durch Rohrleitungen, Dr.diss, RWTH, Westdeutscher Verlag, ISBN 3-531-02456-6, 132 p. + 92 p. fig/tab
Sakuta M., Kasanu I., Yamane S., Sakamoto A. (1989), Pumpability of fresh concrete, Takenaka Technical Research laboratory, Tokyo, pp. 125-133 (ref 50 in Kaplan 2001)
Sedran T., de Larrard F (1999) Optimization of self compacting concrete thanks to packing model, Proceedings 1st SCC Symp, CBI Sweden, RILEM PRO7, 321-332
Smeplass S. (1998) Pumpability of LWA concrete with impregnated, pre-wetted and untreated LWA, Report STF22 A98751, Sintef,(In Norwegian) 28 p.
Smeplass S.(2004) Betongproporsjonering, Utdelt Materiale (UM) 4, Skanska/NTNU fag TKT 4215 Betongteknologi 1 34 s.
Smeplass S. (2008) April 11, pers. Comm., Trondheim, Norway

Spiratos N., Pagé M., Mailvaganam N., Malhotra V.M., Jolicoeur C.(2003) Superplasticizers for Concrete : Fundamentals, Technology, and Practice, Ottawa, ISBN 0-9731507-1-8, 322 p.
Stephenson T.O., Concrete pumping Pumpable concrete, Australian civil Engineering 5 June (1968) 24-27
Tattersall G.H., Banfill P.F.G.(1983) The Rheology of Fresh Concrete, Pitman Books Ltd., London, 356 p.
Tattershall G.H.(1976) The workability of concrete, Viewpoint Publications, Cement and Concrete Association UK, 138 p.
Thrane L.H. (2005) Simulation and verification of form filling with self-compacting concrete, Nordic Concrete Research Publ. No.33, ISBN 82-91341-91-5, 89-91
Thrane L.H.(2007) Form Filling with SCC, Concrete Centre DTI/DTU Denmark, 269 p.
Tuutti K.(2007) October 11 - 12, pers. comm. Stockholm, Sweden
Wallevik O.(1990) Rheology of fresh concrete and utilization on concrete with and without silica fume, Dr.ing dissertation 1990:45 Norw.Univ.Sc.&Tech, 182 p. (In Norw.)
Wallevik O., Gjørv O.E.(1990) Development of a coaxial cylinders viscosimeter for fresh concrete, Proc RILEM Int conference on properties of fresh concrete, 213-224
Wallevik O.(2002) Pumping of concrete, in "Rheology course, IBRI Concrete Industry, Rheology of cement suspensions", Practical applications, Iceland, 623-627
Wallevik J.E.(2003) Rheology of particle suspensions. Fresh concrete, mortar and cement paste with various types of lignosulfonates, Dr.ing dissertation 2003:18 Norw.Univ.Sc.&Tech, 397 p
Wallevik J.E.(2006) Relationship between the Bingham parameters and slump, Cement and Concrete Research (36) 1214-1221
Watanabe K., Kuroiwa S., Ono H., Tanigawa Y.(2001) Evaluation of pumpability of high-fluidity concrete, Consec 01, Univ of BC, Canada, ISBN 0-88865-792-7, Vol.2, 1642-1649
Watanabe K., Ono H., Katou K. and Tanigawa Y.(2007) Analytical and experimental study on flow of fresh concrete in conveying pipe, 5th Int. symp. on SCC, Rilem PRO54 ISBN 978-2-35158-047-9, Vol.1, 393-398
Welty JR, Wicks CE, Wilson RE, Rorrer GL (2001) Fundamentals of momentum, heat and mass transfer, 4th ed., John Wiley and Sons, 759 p.
Wiklund J.(2007) Ultrasound Doppler Based In-Line Rheometry, development, validation and application, Doctoral thesis Lund University ISBN 978-91-628-7025-6, 81 p. + 5 papers

Internet:

www.comsol.com
www.fabeko.no
www.maxit-Group.com
www.putzmeister.com
www.schwing.com

APPENDIX 1
No-slip tube flow of Bingham liquid

The high-friction rubber hose wall makes it reasonable to start by assuming no-slip flow. This is also justified by the recommendation (ACI 1998) 3 times higher pressure in rubber tubes than in steel pipes of equal length and dimension.

For a newtonian fluid flowing between a fixed plate with area A and an equal parallel plate at distance y moving at velocity v due to a force F, the shear, $\tau = F/A$. τ is proportional to the shear rate dv/dy:

$$\tau = \eta \dot{\gamma} = \eta \frac{dv}{dy} (or = \eta \frac{dv}{dr} (tube - geometry)) \quad \text{(A1)}$$

τ: shear [Pa]

$\dot{\gamma}, \frac{dv}{dy}, \frac{dv}{dr}$: rate of shear [$s^{-1}$]

η: viscosity [Pa·s]

v: maximum flow rate equal to speed of moving plate [m/s]

r: radius (m)

y: distance from surface (m)

For a Bingham fluid like concrete there is a yield shear that must be exceeded whereafter the shear is proportional to the rate of shear:

$$\tau = \tau_0 + \mu \frac{dv}{dr} \quad \text{(A2)}$$

τ_0: yield shear strength [Pa]

μ: plastic viscosity [Pa·s]

Then we look at mechanical equilibrium of a cylindrical element of a Bingham fluid:

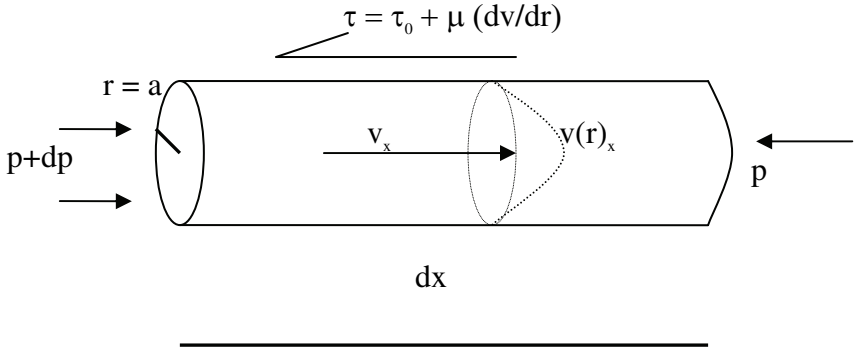

Figure A1: Simplified cylindrical element with uni-axial pressure difference

p: pressure [Pa]

x: length [m]

v_x: total concrete flow [m/s]

v(r): concrete flow as function of radius [m/s]

a: radius of pipe [m]

τ: shear in flowing concrete [Pa], τ assumed > τ_0 at infinitesimal distance from pipe wall and inwards

Mechanical equilibrium along the x-axis of the pipe element in figure A1 requires: $\Sigma F_x = 0$:

$$\pi r^2 dp - 2\pi r dx(\tau_0 + \mu\frac{dv}{dr}) = 0 \qquad \text{(A3)}$$

$$\frac{r}{2}\frac{dp}{dx} - \tau_0 - \mu\frac{dv}{dr} = 0 \qquad \text{(A4)}$$

The velocity distribution v(r) as the fluid flows through a pipe with radius a is found by separating and integrating (A4) with boundary condition v(a) = 0 (no slip):

$$v(r) = \int dv = \frac{1}{2\mu}\frac{dp}{dx}\int r dr - \frac{\tau_0}{\mu}\int dr \qquad \text{(A5)}$$

Plug flow with Bingham slip layer

For a Bingham fluid the cylindrical volume element can only start to move in a tube when the shear-stress $\tau > \tau_0$. For a no-slip condition this means that the cylindrical element in Figure A1 will start to move near the pipe wall like a plug with radius R_0 since the resulting shear load will be largest there, see Fig. A2:

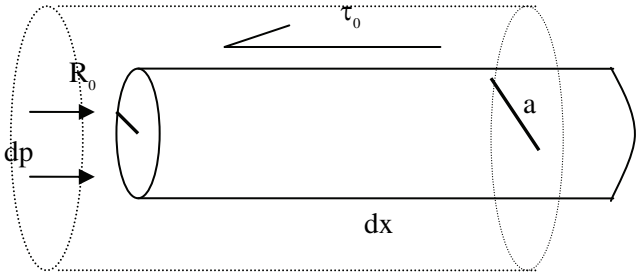

Figure A2: Plug with radius R_0 as shear load from pump pressure exceeds the yield τ_0.

Mechanical equilibrium in the x-direction gives the radius of the plug, R_0 :

$$\pi R_0^2 dp - 2\pi R_0 dx\,\tau_0 = 0 \Rightarrow R_0 = \frac{2\tau_0}{(dp/dx)} \qquad \text{(A6)}$$

R_0: plug radius [m]

The integration of eq.(A5) must therefore give a flow distribution that includes the plug. With positive pressure gradient in the flow direction (A5) becomes:

$$v(r) = \frac{(a^2 - r^2)}{4\mu}\frac{dp}{dx} - \frac{\tau_0}{\mu}(a - r) \qquad r \bullet R_0$$

$$v(r) = v(R_0) \qquad r \bullet R_0 \qquad \text{(A7)}$$

Eq.(A7) does not allow any transport if $R_0 \bullet a$. If there is transport in such a case it is highly probable that the concrete is flowing through the pipe more or less like a plug with a lubricating slippage layer between the plug and the pipe wall. The rheological properties of the layer are different from those of the bulk concrete. Visual inspection of the output from the hose-end in such cases has sometimes revealed a moist surface of a plug-like material. In general there seems, however, to be transitions between plug-like and flow-profile like output. Detailed studies (Kaplan 2001) show that the plastic viscosity of the slippage layer describes the plug flow better than yield shear strength of this fluid layer. Here we shall treat this in a simplified manner by estimating the layer thickness and assuming that it has Bingham behaviour.

The total (integrated) flow, G_x [m^3/s] is obtained from (A7) by multiplication of the plug contribution ($v(R_0)$) and integration of the rest of the cross section between the plug and the pipe wall ($v(R_0)$ to v(a)):

$$G_x = v(R_0)\pi R_0^2 + \int_{R_0}^{a}\left[\frac{(a^2 - r^2)}{4\mu}\frac{dp}{dx} - \frac{\tau_0}{\mu}(a - r)\right]2\pi r dr \qquad \text{(A8)}$$

The resulting total flow, the so-called Buckingham-Reiner equation (Tattersall & Banfill 1983) can, after integration and some algebra, be written (Kaplan 2001):

$$G_x = \frac{\pi a^4}{8\mu}\frac{dp}{dx}\left[1 - \frac{4}{3}\left(\frac{2\tau_0}{a(dp/dx)}\right) + \frac{1}{3}\left(\frac{2\tau_0}{a(dp/dx)}\right)^4\right] = \frac{\pi a^4}{8\mu}\frac{dp}{dx}\left[1 - \frac{4R_0}{3a} + \left(\frac{R_0}{3a}\right)^4\right] \qquad \text{(A9)}$$

R_0 is given by equation (A6). The flow velocity, v_x [m/s], is:

$$v_x = \frac{1}{\pi a^2}G_x \qquad \text{(A10)}$$

Eq.(A7) and (A9) normally underestimate concrete flow. However, by evaluating R_0 from eq.(6) and calculating the flow profiles and total flow with eq.(A7) and (A9) one can assess whether a concrete is far from, or close to plug flow. One may then simply fit the total flow to an estimated plug radius $R_{0\,est}$. This means estimating the layer thickness ($a\text{-}R_{0\,est}$) and adjusting the rheological properties of the slip layer, $\tau_{0,SL}$ and μ_{SL} to some properties more viscous than of the bulk fresh concrete (τ_0, μ). One may also calculate the specific plastic viscosity and yield shear of the slip layer: $\tau_{0,SL\,spec} = \tau_{0,SL}/(a\text{-}R_0)$ and $\mu_{SL\,spec} = \mu_{SL}/(a\text{-}R_0)$ but perhaps even better; to use a slip layer equivalent visco-thickness coefficient: $(a\text{-}R_0)^2/\mu_{SL}$. Important further work will be to obtain experimental data on the existence, possible thickness and rheological properties of the slip layer.

APPENDIX 2
The Navier Stokes equation

Hydrostatic equilibrium of a fluid at rest is described from the mass force in equilibrium with hydrostatic pressure:

$$-\frac{1}{\rho}\nabla p + f = 0 \qquad \text{(A11)}$$

f: mass force vector [N/kg =m/s^2]
ρ: fluid density [kg/m^3]
∇p: gradient of the pressure vector [Pa/m] $\nabla p = i\frac{\partial p_x}{\partial x} + j\frac{\partial p_y}{\partial y} + k\frac{\partial p_z}{\partial z}$ and *i,j,k* unit vectors in x-, y- and z-directions (=dp/dx for uniaxial case)

Eulers equation describes the flow of an ideal fluid in motion without friction and can be solved together with the continuity equation for an incompressible fluid:

$$\frac{\partial v}{\partial t} = -\frac{1}{\rho}\nabla p + f - (v\cdot\nabla)v \quad \text{with} \quad \frac{\partial \rho}{\partial t} + \nabla\cdot(\rho v) = 0 \qquad \text{(A12)}$$

v: velocity vector [m/s]
t: time [s]
$v\cdot\nabla$: convection differentiate [1/s], $v\cdot\nabla = v_x\frac{\partial}{\partial x} + v_y\frac{\partial}{\partial y} + v_z\frac{\partial}{\partial z}$

Differentiating the product $\nabla\cdot(\rho v) = v_x\frac{\partial \rho}{\partial x} + v_y\frac{\partial \rho}{\partial y} + v_z\frac{\partial \rho}{\partial z} + \rho\frac{\partial v_x}{\partial x} + \rho\frac{\partial v_y}{\partial y} + \rho\frac{\partial v_z}{\partial z}$

Introducing the friction within the liquid due to the viscous behaviour results in Navier Stokes equation:

$$\frac{\partial v}{\partial t} = -\frac{1}{\rho}\nabla p + f - (v\cdot\nabla)v + \frac{\mu}{\rho}\nabla^2 v \qquad \text{(A13)}$$

∇^2 is the Laplace operator so that $\nabla^2 v = \frac{\partial^2 v_x}{\partial x^2} + \frac{\partial^2 v_y}{\partial y^2} + \frac{\partial^2 v_z}{\partial z^2}$ [1/ms] and μ/ρ: [m^2/s]

Note that using (A13) with cylindrical coordinates for the uniaxial simple case in figure A1 one can arrive at eq. (A4). In numerical solutions of (A13) using commercial FEM-software, we may introduce other rheological models, thus solving for non-newtonian fluids.

Appendix 3 Excel sheet solving Buckingham Reiner – example figure 16

Velocity distribution over hose with no-slip plug flow, plug-radius R_0 (Hagen Poiselle Bingham flow, which integrated -> Buckingham Reiner equation (Tatt&Ban 1983, Kaplan 2001)):

$v(r) = -((a^2-r^2)/4\mu)\cdot(dp/dx) - \tau_o/\mu\,(a-r)$, $r \geq R_0$ and $v(R_0)$, $r \leq R_0$, $R_0 = 2\tau_0/(dp/dx)$

(r = a ved rand)

cells for entering variables

NB: error at R_0 > a

Material: ND Ref 8mm 60MPa Diameter: 45 mm

$v(r)_{no\text{-}plug}$	r	dp/dx	a	τ_0	μ	R_0
(m/s)	(mm)	(Pa/m)	(mm)	Pa	Pa·s	(mm)
0,00	22,5	29962,4	22,5	57	8,57	3,8
0,05	21			(bulk concrete)		
0,09	19,5					
0,13	18					
0,16	16,5					
0,20	15					
0,22	13,5					
0,25	12					
0,27	10,5					
0,28	9					
0,29	7,5					
0,30	6					
0,31	4,5					
0,31	3					
0,31	1,5					
0,31	0					
0,31	-1,5					
0,31	-3					
0,31	-4,5					
0,30	-6					
0,29	-7,5					
0,28	-9					
0,27	-10,5					
0,25	-12					

$\tau_0 = 57$ Pa, $\mu = 8.6$ Pa.s, Ø = 45 mm, L= 26,6 m, dp/dx = 30 kPa/m

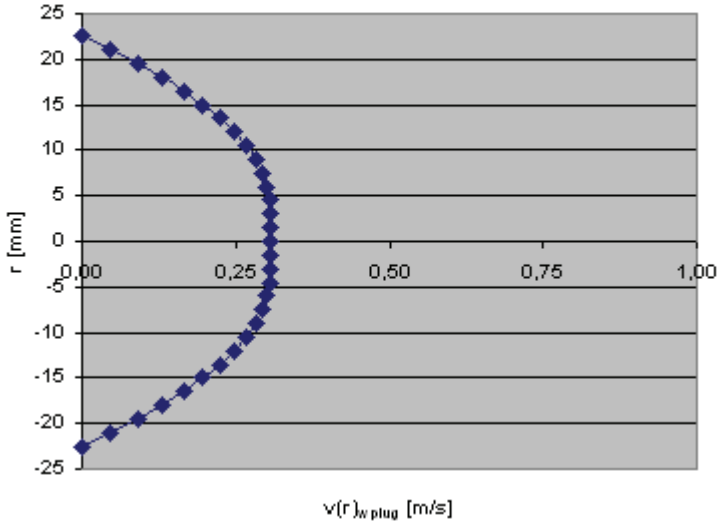

a (total hose radius)		BML plast.visc. μ	Measured press. dp (over 26,6 m hose)	BML yield str τ_o	$R_{plug}=(2L/\Delta p)\tau_0$	v_x meas.	G_x meas.		
m		Pa.s	Pa	Pa	mm	m/s	lit/s		
0,015	EXM m-Tec	16,5	30000	4,4	**8**	**0,28**	0,20		
0,015	EXM batch	14,2	170000	13,3	**4**	**0,27**	0,19		
0,015	JMS m-Tec	25,5	2000000	873	**23**	**0,25**	0,18	**G (lit/s)**	**v_x (m/s)**
0,015	JMS batch	23,1	2000000	875	**23**	**0,23**	0,16	**0,27**	**0,17**
0,015	REP m-Tec	21,4	100000	130	**69**	**0,25**	0,18		
0,015	REP batch	7,4	10000	55	**293**	**0,25**	0,18		
0,0225	Reference 4mm 30 MPa	3,7	735000	146,05	**11**	**0,42**	0,67		
0,0225	Reference 4mm 60 MPa	5,78	726000	144,81	**11**	**0,66**	1,05		
0,0225	Reference 8mm 30 MPa	2,05	476000	61,42	**7**	**0,71**	1,13		
0,0225	Reference 8mm 60 MPa	8,57	797000	57,05	**4**	**0,60**	0,95		
0,0225	LWA 4mm 30 MPa	4,6	332000	228,49	**37**	**0,89**	1,42		
0,0225	LWA 4mm 60 MPa	2,7	489000	82,74	**9**	**0,41**	0,66		
0,0225	LWA 8mm 30 MPa	1,33	283000	21,82	**4**	**0,64**	1,01		
0,0225	LWA 8mm 60 MPa	0,98	293000	5,59	**1**	**0,92**	1,47		
0,0225	maxit ton 915 m-tec	2,66							

FLOW SUMMED FROM PROFILE:

G_x (lit/s)	
0,272486973	
0,004822882	
0,013095476	
0,019398167	
0,023897769	
0,026761096	
0,028154961	
0,028246179	
0,027201562	
0,025187925	

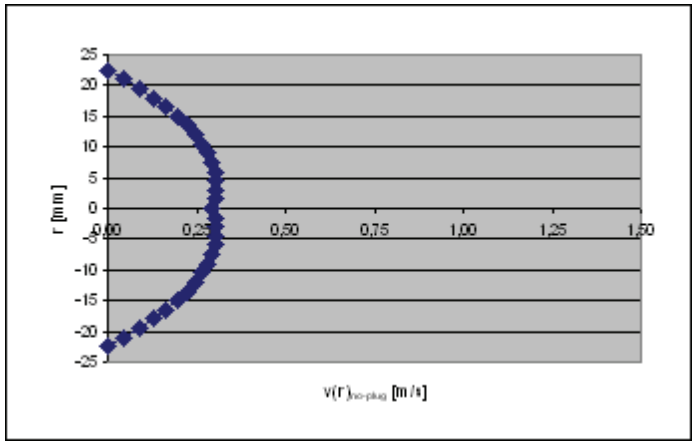

Appendix 4 Excel sheet for plug flow with adjustable slip layer – modified Buckingham Reiner – figure 17, 21, 22

Velocity distribution in hose with plug-flow and slip-layer. Plug-radius R_0 fitted to measured flow by estimateing layer thickness (a-R_0), yield and plastic viscosity of slip-layer

$v(r) = -((a^2-r^2)/4\mu)\cdot(dp/dx) - \tau_o/\mu\,(a-r)$, $r \geq R_0$ and $v(R_0)$, $r \leq R_0$, R_0 estim, not $2\tau_0/(dp/dx)$

(r = a at wall)

cells for entering variables

$R_{0\,est}$ = (a- 2,1) mm (tube rad. - slip layer thickn.)

NB: error at R_0 > a

Material: ND Ref 8mm 60MPa Diameter: 45 mm

$v(r)_{no\text{-}plug}$	r	dp/dx	a	$\tau_{0\,SL}$	μ_{SL}	$R_{0\,est}$ =	$v(r)_{plug}$	r
(m/s)	(mm)	(Pa/m)	(mm)	Pa	Pa·s	(mm)		(mm)
0,00	22,5	29962,4	22,5	2	1	20,4	0,00	22,5
0,49	21			(Slip Layer)			0,49	21
0,94	19,5						0,67	19,5
1,36	18						0,67	18
1,74	16,5						0,67	16,5
							0,67	15
							0,67	13,5
							0,67	12
							0,67	10,5
							0,67	9
							0,67	7,5
							0,67	6
							0,67	4,5
							0,67	3
							0,67	1,5
							0,67	0
							0,67	-1,5
							0,67	-3
							0,67	-4,5
3,49	-6						0,67	-6
3,34	-7,5						0,67	-7,5
3,16	-9						0,67	-9
2,94	-10,5						0,67	-10,5
2,69	-12						0,67	-12

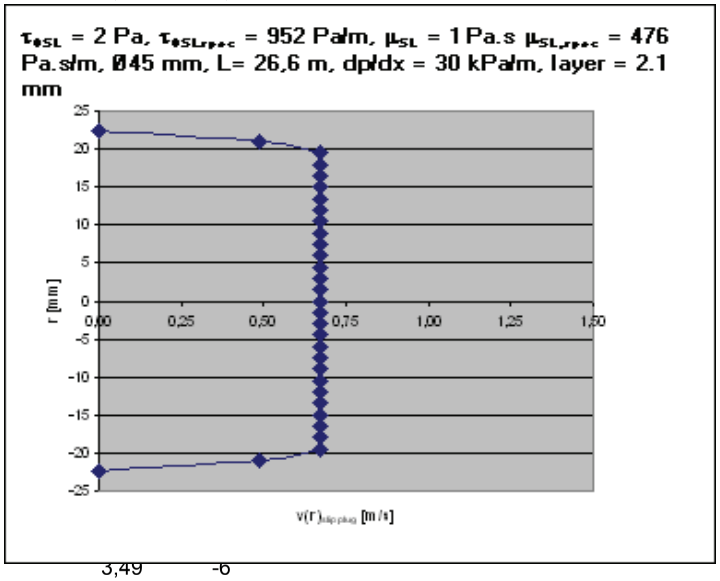

	BML plast.visc. μ Pa.s	Measured press. dp (over 26,6 m hose) Pa	BML yield str τ_o Pa	$R_{plug}=(2L/\Delta p)\tau_0$ mm	v_x meas. m/s	G_x meas. lit/s	G (lit/s)	v_x (m/s)
0,015 EXM m-Tec	16,5	30000	4,4	**8**	**0,28**	0,20		
0,015 EXM batch	14,2	170000	13,3	**4**	**0,27**	0,19		
0,015 JMS m-Tec	25,5	2000000	873	**23**	**0,25**	0,18	**G (lit/s)**	**v_x (m/s)**
0,015 JMS batch	23,1	2000000	875	**23**	**0,23**	0,16	**0,95**	**0,60**
0,015 REP m-Tec	21,4	100000	130	**69**	**0,25**	0,18		
0,015 REP batch	7,4	10000	55	**293**	**0,25**	0,18		
0,0225 Reference 4mm 30 MPa	3,7	735000	146,05	**11**	**0,42**	0,67		
0,0225 Reference 4mm 60 MPa	5,78	726000	144,81	**11**	**0,66**	1,05		
0,0225 Reference 8mm 30 MPa	2,05	476000	61,42	**7**	**0,71**	1,13		
0,0225 Reference 8mm 60 MPa	8,57	797000	57,05	**4**	**0,60**	0,95		
0,0225 LWA 4mm 30 MPa	4,6	332000	228,49	**37**	**0,89**	1,42		
0,0225 LWA 4mm 60 MPa	2,7	489000	82,74	**9**	**0,41**	0,66		
0,0225 LWA 8mm 30 MPa	1,33	283000	21,82	**4**	**0,64**	1,01		
0,0225 LWA 8mm 60 MPa	0,98	293000	5,59	**1**	**0,92**	1,47		
0,0225 maxit ton 915 m-tec	2,66	529000	96,19	**10**	**0,64**	1,01		

TOTAL FLOW AND VELOCITY OF ESTIMATED PLUG SHAPE:

G_x (lit/s) **0,96126** **v_x (m/s)** **0,60**

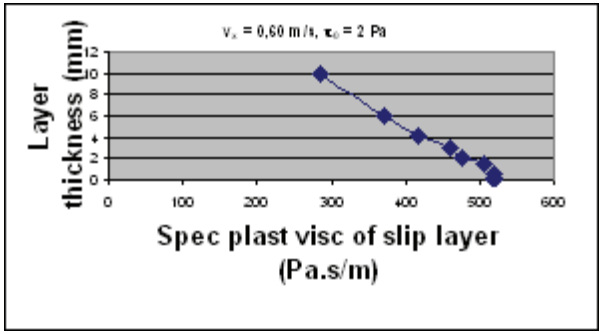

476,1905Pa·s/m

$\mu_{SL,spec}$ Pa·s/m	(R0-a) mm	
285	10	
372	6	
417	4,2	
460	3	(limit due to simplified integration?)

Appendix 5 2D Numerical simulation: Modified Bingham Model - Papanastasiou Model

EXM m-Tec

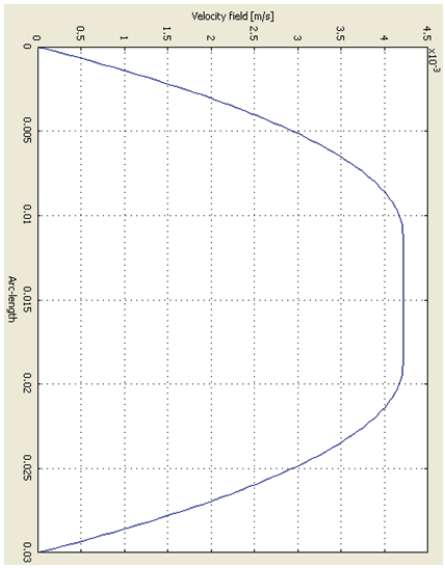

EXM batch

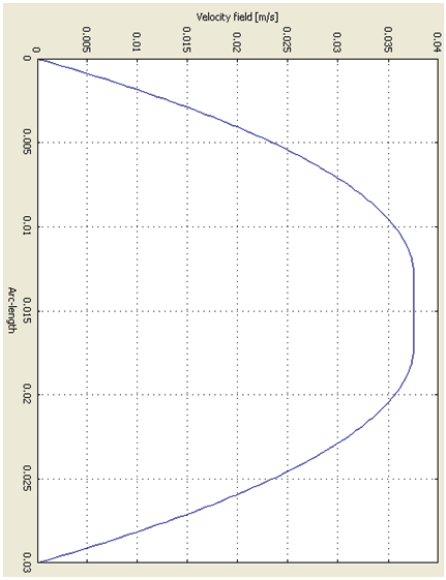

JMS m-Tec

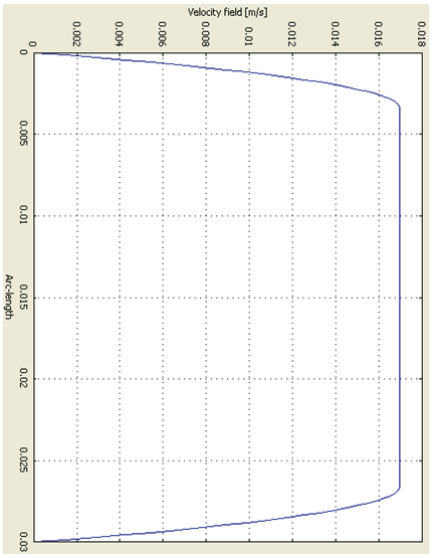

JMS batch

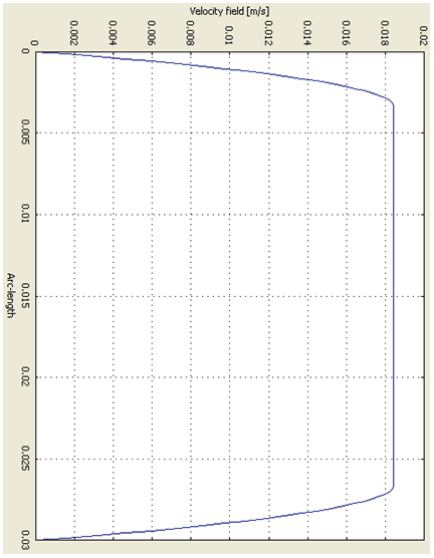

REP m-Tec

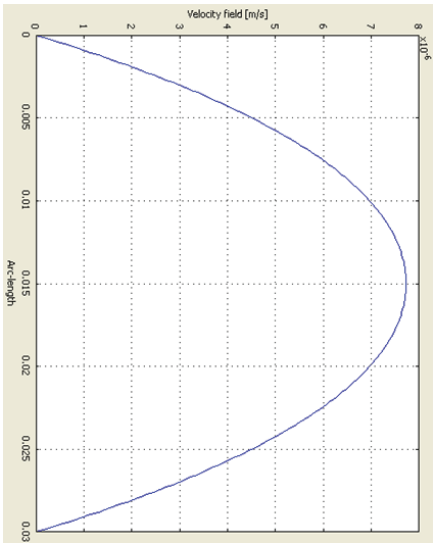

Ref 4mm30MPa

REP batch

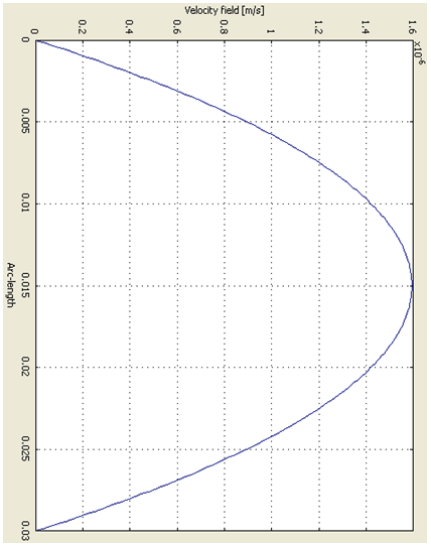

Ref 4mm 60MPa

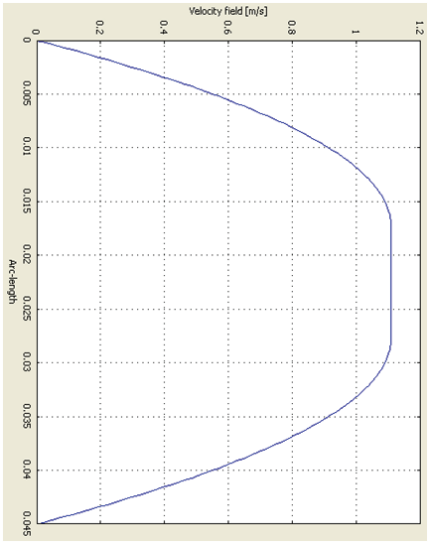

Ref 8mm 30MPa

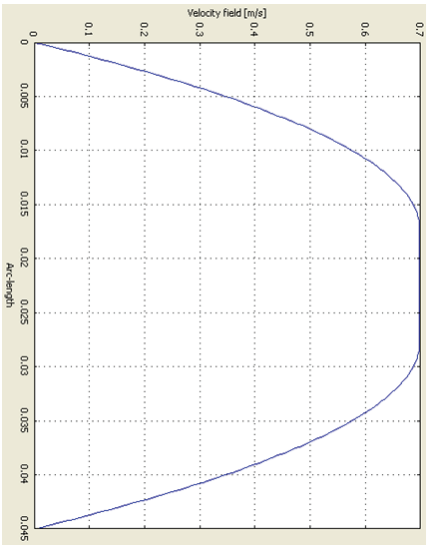

Ref 8mm 60MPa

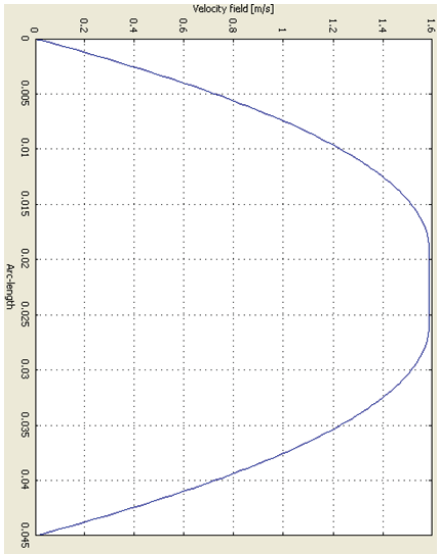

LWA 4mm 30MPa

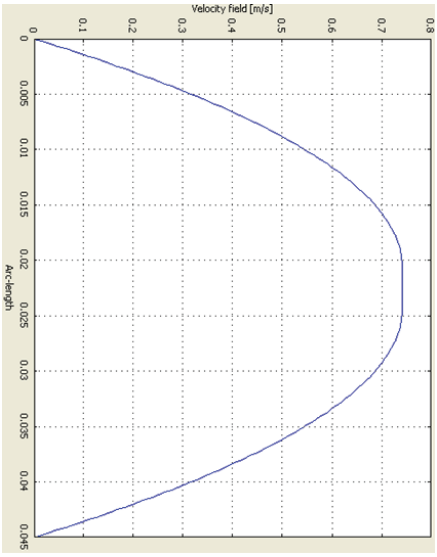

LWA 4mm 60MPa

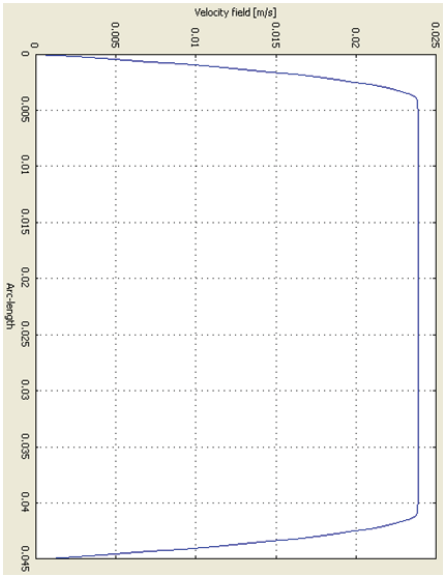

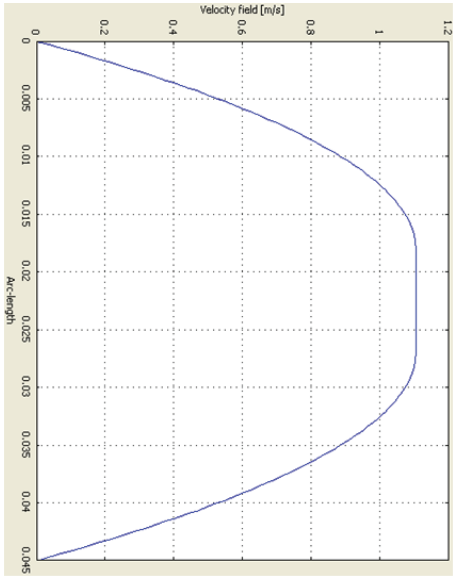

LWA 8mm 30MPa

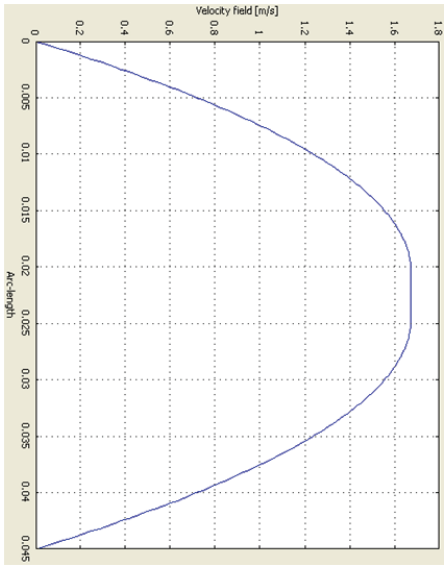

LWA 8mm 60MPa

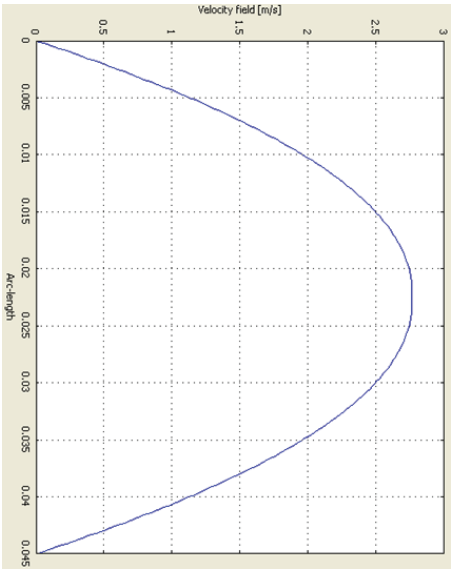

Maxit ton 915 m-Tec

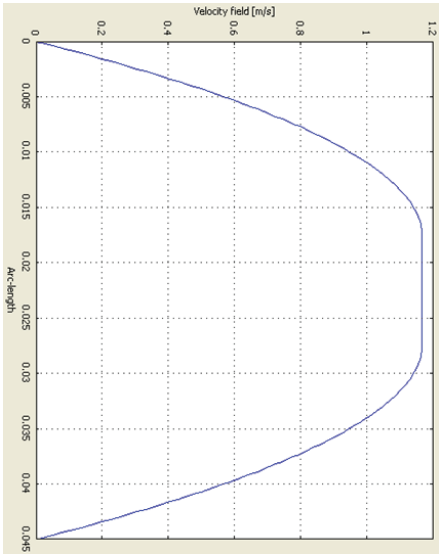

SINTEF Building and Infrastructure is the third largest building research institute in Europe. Our objective is to promote environmentally friendly, cost-effective products and solutions within the built environment. SINTEF Building and Infrastructure is Norway's leading provider of research-based knowledge to the construction sector. Through our activity in research and development, we have established a unique platform for disseminating knowledge throughout a large part of the construction industry.

COIN – Concrete Innovation Center is a Center for Research based Innovation (CRI) initiated by the Research Council of Norway. The vision of COIN is creation of more attractive concrete buildings and constructions. The primary goal is to fulfill this vision by bringing the development a major leap forward by long-term research in close alliances with the industry regarding advanced materials, efficient construction techniques and new design concepts combined with more environmentally friendly material production.